UNIVERSIDADE FEDERAL DA PARAÍBA
CENTRO DE ENERGIAS ALTERNATIVAS E RENOVÁVEIS
PROGRAMA DE PÓS-GRADUAÇÃO EM ENGENHARIA ELÉTRICA

Dissertation Exam

ANALYSIS OF THE IMPACT OF THE INSERTION OF DISTRIBUTED GENERATION IN THE ELECTRIC GRID BASED ON IMPEDANCE, VOLTAGE AND POWER FACTOR

Maria Cecilia Costa Lima

João Pessoa, Brazil
February 2021

Maria Cecilia Costa Lima

ANALYSIS OF THE IMPACT OF THE INSERTION OF DISTRIBUTED GENERATION IN THE ELECTRIC GRID BASED ON IMPEDANCE, VOLTAGE AND POWER FACTOR

Dissertation exam presented to the Programa de Pós Graduação em Engenharia Elétrica - PPGEE, from the Universidade Federal da Paraíba - UFPB, as a partial requirement to obtain the title of Master in Electrical Engineering.

Advisors: Dr. Fabiano Salvadori
Dra. Camila S. Gehrke

João Pessoa, Brazil

February 2021

Catalogação na publicação
Seção de Catalogação e Classificação

L732a Lima, Maria Cecília Costa.
Analysis of the impact of the insertion of distributed generation in the electric grid based on impedance, voltage and power factor. / Maria Cecília Costa Lima. - João Pessoa, 2021.
51 f. : il.

Orientação: Fabiano Salvadori.
Coorientação: Camila Seibel Gerhke.
Dissertação (Mestrado) - UFPB/CEAR.

1. Electrical Engineering - Distributed generation. 2. Power factor analysis. 3. Sensitivity indexes. 4. Renewable sources. 5. Overvoltage analysis. I. Salvadori, Fabiano. II. Gerhke, Camila Seibel. III. Título.

UFPB/BC CDU 621(043)

Elaborado por WALQUELINE DA SILVA ARAUJO - CRB-15/514

ACKNOWLEDGEMENTS

I thank God for giving me the strength, knowledge and calm to not give up during these two years, which have proven to be the hardest of my life so far.

To my family, mom, dad and Luiza, for being my source of support, for always believing in me, encouraging me to follow my goals and dreams, and teaching me since I was a child that nothing is impossible if you have the will and determination necessary. I wouldn't be the person I am today without your guidance, and I definitely would not have made it this far without you. Thank you for everything. I love you.

To my coleagues of Master's, who shared some of the doubts, uncertanties and were by my side, even those who for many reasons couldn't complete the two years. A special thank you to my friend Laysa, whom I met during a class, and intend to be friends with for the rest of my life.

To my best friend for life, who I met during the undergraduate years and is now a huge part of my life, thank you for the support during the dawns, uncountable hours of conversation, for believing in me even when I didn't, for the knowledge we share even today and for everything you taught and continue teaching me. I love you.

To my advisors Fabiano Salvadori and Camila Gehrke, for the help on the development of this work, the patience to share all the knowledge and for believing in me. Thank you.

UNIVERSIDADE FEDERAL DA PARAÍBA – UFPB
CENTRO DE ENERGIAS ALTERNATIVAS E RENOVÁVEIS – CEAR
PROGRAMA DE PÓS-GRADUAÇÃO EM ENGENHARIA ELÉTRICA - PPGEE

A Comissão Examinadora, abaixo assinada, aprova a Dissertação

ANALYSIS OF THE IMPACT OF THE INSERTION OF DISTRIBUTED GENERATION IN THE ELECTRIC GRID BASED ON IMPEDANCE, VOLTAGE AND POWER FACTOR

Elaborada por

MARIA CECILIA COSTA LIMA

como requisito parcial para obtenção do grau de

Mestre em Engenharia Elétrica.

COMISSÃO EXAMINADORA

PROF. DR. FABIANO SALVADORI
Orientador – UFPB

PROFª. DRª. CAMILA SEIBEL GEHRKE
Examinador Externo – UFPB

PROF. DR. FRANKLIN MARTINS PEREIRA PAMPLONA
Examinador Externo – IFPB

PROF. DR. MARCEL AYRES DE ARAÚJO
Examinador Externo – UFRPE

João Pessoa/PB, 22 de fevereiro de 2021

ABSTRACT

This work consists of an analysis of the sensitivity of points of common coupling (PCCs) against the insertion of distributed generation (DG), by modeling circuits based on Kirchhoff's Laws, Ohm's Law, admittance matrix and using sources of ideal currents that characterize the DG to propose sensitivity indexes for voltage and impedance of each PCC. This study evaluates the influence of DG on the voltage levels of systems with 16 PCCs, calculating the admittance matrix of this system in the MATLAB software. Variations in the load, in the grid impedance and in the power factor (PF) of the DGs were considered to evaluate voltage variations. The results show the analysis of the impact of the DGs on the grid without the need to perform simulations, using the indexes proposed.

Keywords: Distributed Generation, Power Factor Analysis, Sensitivity Indexes, Renewable Sources, Overvoltage Analysis.

LIST OF FIGURES

LIST OF TABLES

LIST OF ABBREVIATIONS AND ACRONYMS

ABSOLAR	*Associação Brasileira de Energia Solar Fotovoltaica*
ANEEL	*Agência Nacional de Energia Elétrica*
DG	Distributed generation
EPQ	Electric power quality
IEC	International Electrotechnical Commission
ISI	Impedance Sensitivity Index
LKC	Lei de Kirchhoff das Correntes
LKT	Lei de Kirchhoff das Tensões
MPPT	Maximum power point tracker
NBR	*Norma Brasileira*
NDU	*Norma de Distribuição Unificada*
ONS	*Operador Nacional do Sistema*
PCC	point of common coupling
PF	Power Factor
PFSI	Power Factor Sensitivity Index
PRODIST	*Procedimentos de Distribuição de Energia Elétrica no Sistema Elétrico Nacional*
PV	Photovoltaic
QEE	*Qualidade de Energia Elétrica*
SDVV	Short Duration Voltage Variation
SIN	*Sistema Interligado Nacional*
THD	Total harmonic distortion
VSI	Voltage Sensitivity Index

CONTENTS

1 INTRODUCTION

For a long time, the electricity delivered to the consumer came only from centralized generation, which consists of large-scale generation and large powers, usually in hydroelectric and thermoelectric plants (Figure 1.1). In the first case, requiring a lot of space for its construction, resulting in flooding of large areas, displacement of the riverside population and eventual change in the aquatic habitat in the region of installation. In the case of thermoelectric plants, fossil fuels are burned, causing great environmental damage in the long and short term.

Figure 1.1 – Traditional electricity delivery system - centralized generation.

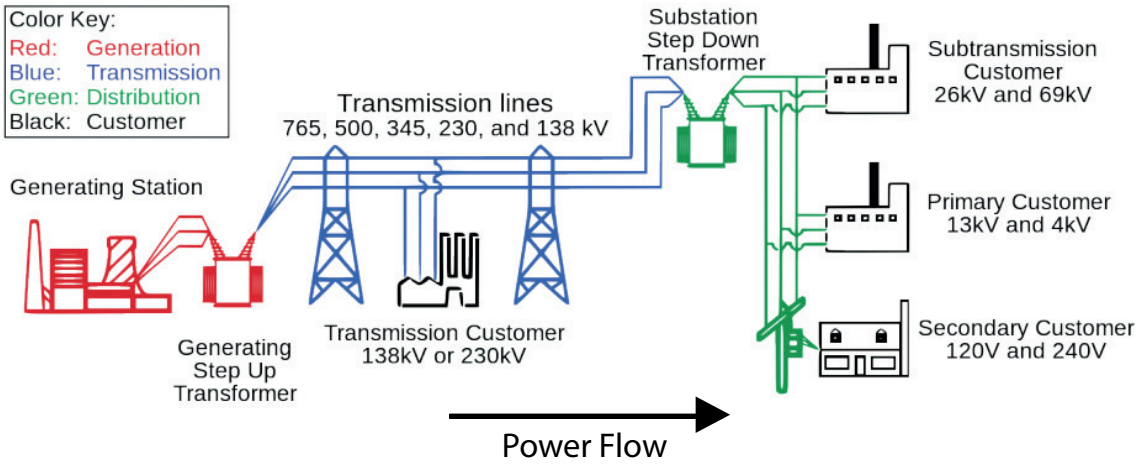

Source: Department of Energy - USA, 2015.

The brazilian electrical system is based mostly on centralized generation. However, in the beginning of the century blackouts ocurred in Brazil showed the problems that the transmition and distribution systems have and challenged the agents of the electric sector and the consumers themselves to find solutions to those problems. Then there was the creation of the *Sistema Interligado Nacional (SIN)*, linking the generation and distribution of several regions of the country with each other, increasing the reliability of the brazilian electrical system and avoiding significant power outages. In addition, more hydroelectric plants were built and put into operation, which caused an increase in the number of transmission lines that cross the country and the distribution lines between the substations and the final consumer.

The distance between generation and final consumption leads to losses, which depending on the location can be significant. The distribution system, despite being sufficient to meet the basic needs of consumers and to make the electrical system reliable and affordable, cannot meet the current needs for greater resilience, power quality and consumer participation.

Thus, concerns about the environment, the increase in electricity consumption and the depletion of alternatives considered economically and environmentally viable for large hydroelectric generation, has led to the search for alternative sources of energy to diversify the electric matrix, resulting in the evolution of the electric power grid. The process of diversification has been causing changes in the communication and electrical infrastructure, connecting the costumer to the substation, distribution and control center instead of the unilateral communication from system operator to the costumer and the poor electrical infrastructure of the past, as seen on Figure 1.2. Therefore, distributed generation (DG), which consists of the installation of small generators, usually from renewable sources or even using fossil fuels, located close to the centers of electricity consumption (ANEEL, 2021), proved to be a good alternative and has become a great ally of the consumer, since the generation occurs in the place where the electric energy is consumed.

Figure 1.2 – Evolution of the Electric Power Grid.

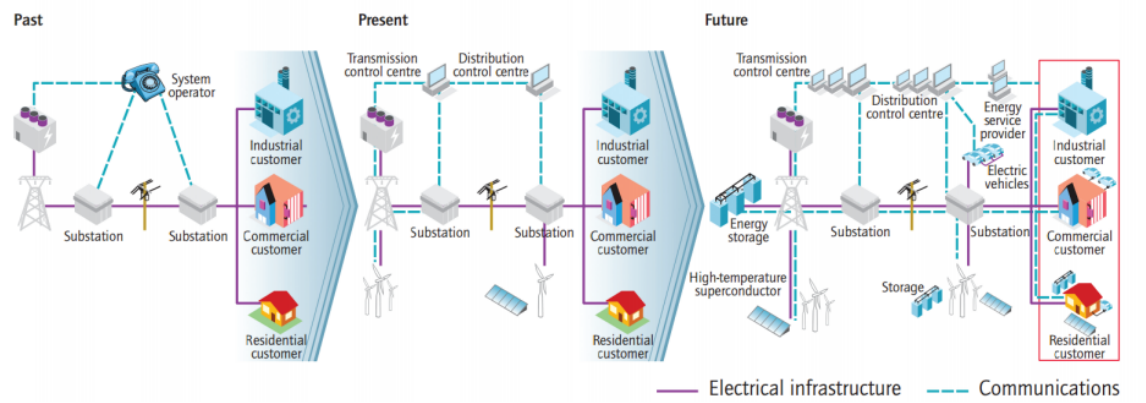

Source: Department of Energy USA. Credit: OECD/IEA 2011 Technology Roadmap: Smart Grids, IEA Publishing.

The DG can present some benefits when interacting to the utility grid, such as low environmental impact, improvement of the voltage level of the grid in periods of high demand, reduction of losses, diversification of the energy matrix and the reduction of expenses with the expansion of transmission lines and distribution networks.

The "REN21 - Renewable Energy for the 21st Century" community provided on its Global Status Report from 2020 the estimated renewable energy share of global energy production, related to the end of 2019, where 27.3% of the energy was generated from renewable energy, such as wind, solar, hydropower, biomass, and others (Figure 1.3). The use of renewable sources has been increasing considerably due to the growth in policy targets of governments, and the higher access to distributed generation from residential and commercial customers. In 2019, more than 200 GW of electric power were added to the power capacity used to supply energy to the consumers. Of those 200 GW, almost 120 GW were added through the use of solar power, and the 80 GW remaining were supplied

using wind power, hydro power, geothermal, ocean power and concentrated solar power (CSP) plants as can be seen on the year 2019 data in Figure 1.4.

Figure 1.3 – Estimated Renewable Share of Global Energy Production - End of 2019.

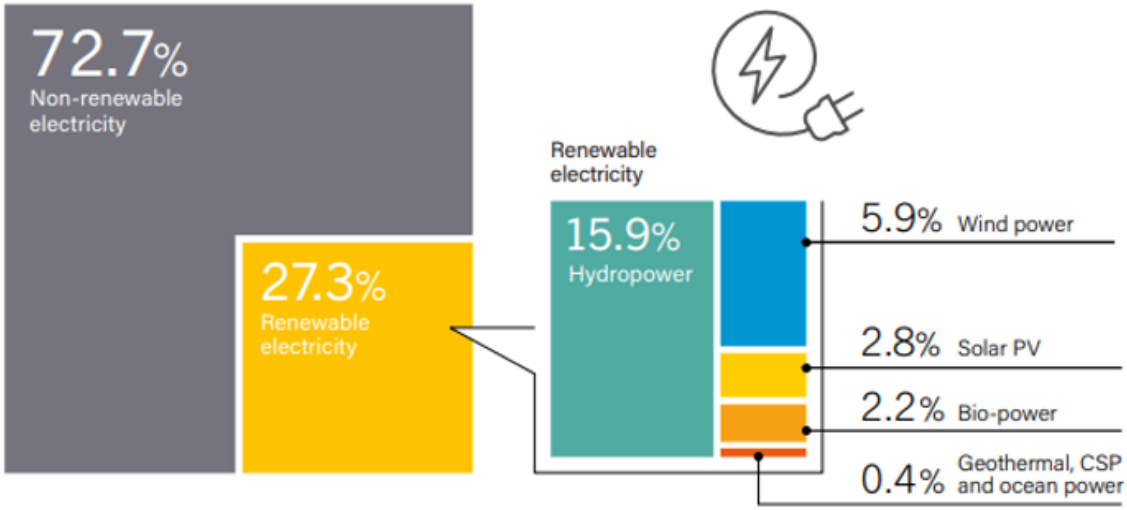

Source: REN 21, 2020.

Figure 1.4 – Annual Additions of Renewable Power Capacity, by Technology and Total, 2013 - 2019.

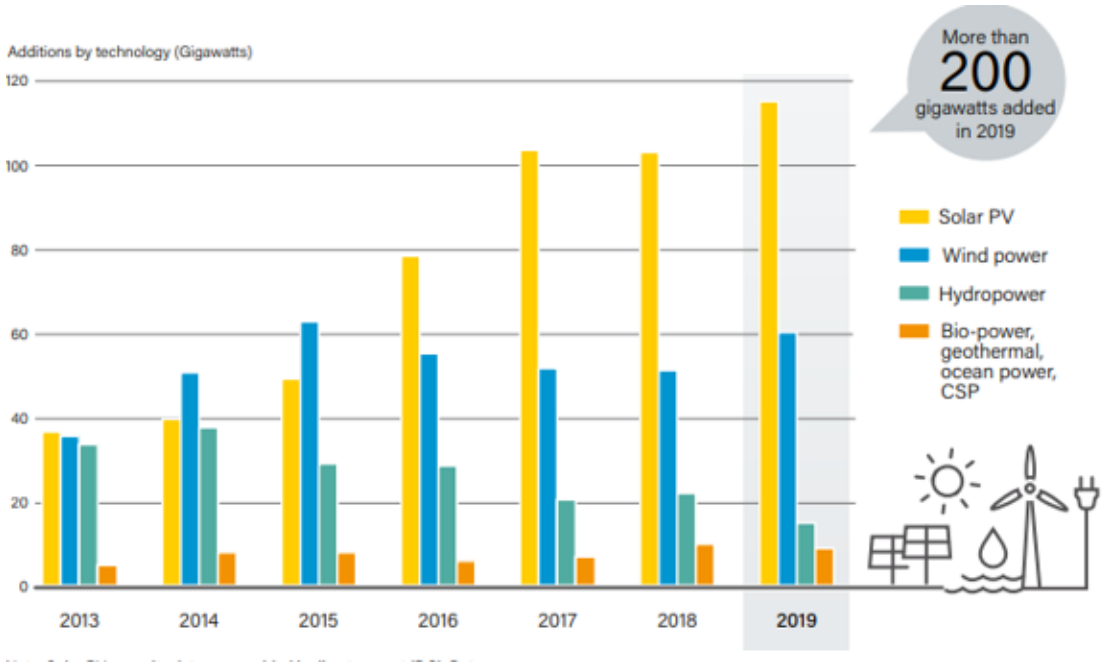

Source: REN 21, 2020.

However, the increase in the insertion of DG in the power grid such as wind generators, photovoltaic systems and energy storage systems (batteries) also has negative aspects, bringing challenges to the managers of the electrical system, such as overvoltage,

low power quality, control and protection problems, which occurs mainly due to the possibility of reverse power flow (WALLING et al., 2008).

The DG can be based on some types of generators, these being synchronous, by induction (both used in wind systems) or using an inverter (most used in photovoltaic systems). A DG with synchronous generator has the capacity to support a high fault current for a longer period of time than a DG with induction generator (SCHWEITZER; FINNEY; V., 2012). In contrast, the fault current of the DG with inverter is limited by the internal control system, and may not be high enough to be detected by the current sensor of the electrical grid and lead to failure in the overcurrent protection system (SHAHZAD; KAHROBAEE; ASGARPOOR, 2017).

The DG must be appropriately coordinated with the operation of the electrical system and the feeder to have a positive role in the areas of power quality, loss reduction and reliability. It is necessary to address issues related to voltage regulation and oscillation, harmonic distortion, islanding, ground compatibility, protection against overcurrent, capacity limits, and other factors. This coordination becomes more critical as the capacity and power of a DG in a circuit is greater than the capacity and demand of the feeder (BARKER; MELLO, 2000).

Regarding voltage levels, the decrease in load at a point where the DG is connected, especially if it is connected in a location distant from the main feeder, is one of the factors that causes overvoltage, while the increase in load demand leads to a drop in the voltage, which can cause undervoltage, that is, voltage at levels below the minimum limits. The bidirectional power flow also interferes with the effectiveness of conventional voltage regulation, which is based on the power flows from the substation to the loads (Figure 1.5). One way to mitigate this problem is to analyze the voltage adjustment with active and reactive power, since the control using the injection of reactive power proved to be an efficient way to guarantee the stability of voltage levels in a distribution network, according to (QI et al., 2018).

Figure 1.5 – Comparison of unidirection power flow and bidirectional power flow.

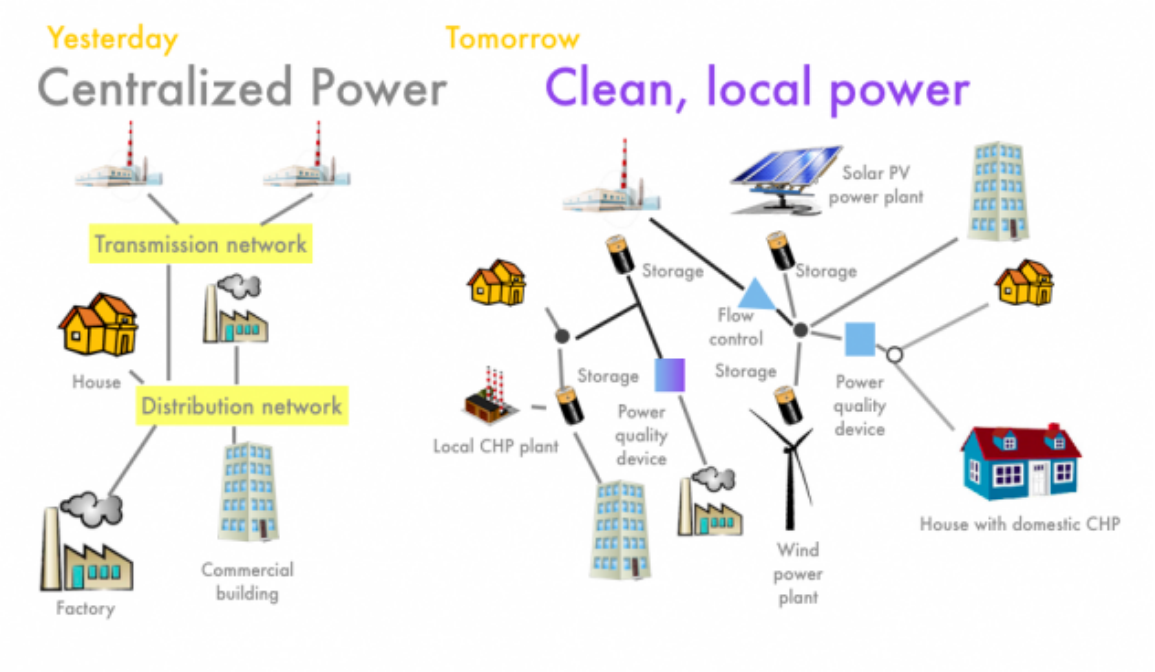

Source: John Farrell - Institute for Local Self-Reliance, 2012.

The commercial inverters of photovoltaic systems have functions such as limitations of injection of active and reactive power, frequency and voltage control in order to meet the requirements and parameters that guarantee the electric power quality (EPQ). The EPQ must be monitored continuously as the photovoltaic generation systems contribute significantly to the injection of reactive power from the grid, through the variation of the DG power factor, which can be caused by climatic changes (rain, variation of solar irradiance). During certain periods of time, distributed solar generation can inject or consume reactive power from the grid in addition to increasing variations in active power consumption (SOUZA et al., 2018).

Given the problems above listed, the analysis of the impacts of the insertion of DG in the network is an extremely important issue nowadays, due to the increase in its use and the challenges it imposes on the operators of the electrical system. As most commercial DG systems operate as a current source, the objective of this work is to analyze the sensitivity of the variation of voltage levels in points of commom coupling (PCCs) of the distribution network to the insertion of DG.

The methodology consists of modeling electrical circuits based on Kirchhoff's and Ohm's Laws, impedance matrix and use of ideal current sources that represent the DG, to propose indexes based on the voltage and impedance of each PCC, determining which points of the circuits are more receptive to install DG with greater power and which points are more sensitive to installation. For this study, voltage, impedance and power factor of the DG are used as parameters, since the main goal of this work is to develop indexes that

indicate the sensitivity using easily obtainable variables.

1.1 MOTIVATION

To better understand the problems brought by the insertion of DG, it is essential to study and analyze the effects that this connection brings to the grid, its voltages, power factor, and harmonics. Also, the benefits that the DG brings to the grid, such as voltage control, and ancillary services, as the increasing number of distributed generation (wind generators, photovoltaic systems, energy storage systems, electric cars) that have been incorporated continuously into the electrical network must meet the requirements established in standards responsible for ensuring the maintenance of EPQ, voltage limits and reliability of the electrical power system. However, as most of the works found in the literature deal with studies with several variables such as power flow, measurements in real networks as will be seen in the bibliographic review, this work seeks a more straightforward, yet still relevant, way of analyzing the impacts of DG in the network, reducing the disadvantages of the research methodology and facilitating the process.

1.2 PURPOSE

1.2.1 General purpose

The purpose of this work is to analyze the impacts of the insertion of DG systems on the sensitivity of PCCs of the electric network, proposing indexes based on impedance, analysis of voltage levels and variation of the power factor of the DGs connected to the network.

1.2.2 Specific purposes

- Modeling the electrical system based on the creation of an admittance matrix;
- Study of the equivalent impedance of PCCs in the electrical system;
- Determination of current amplitude values that represent the DG for performing voltage level compensation;
- Variation of load and line values of the distribution network based on the Monte Carlo simulation method;
- Analysis of the most sensitive points to the insertion of DG using the impedance and variation of the power factor (PF) of the DG.

1.3 WORK ORGANIZATION

The work is organized as follows: chapter 2 reviews published works on how to analyze the impacts of generation distributed on the electrical grid and the methodology applied for these analyses. Chapter 3 outlines the theoretical foundation on distributed generation, the technical standards and theorems of electrical circuits used in the development of the work. Chapter 4 describes the modeling and analysis of the variation in voltage levels of a circuit representing the electrical network, with 16 PCCs when current sources representing the DG are inserted. Chapter 5 presents the proposed sensitivity indexes, by impedance and voltage, in addition to the analysis of the power factor variation. Chapter 6 presents the results of the analysis of variation of impedance, voltage and power factor and the proposed indexes. Finally, in chapter 7, the work is concluded based on the results obtained.

2 LITERATURE REVIEW

The increased insertion of distributed generation in the electricity grid has been causing some problems that negatively influence the electricity quality, as mentioned before. The challenges imposed by the increased installation of DG require detailed studies and several works in the literature seek the best way to analyze the impacts of DG on the distribution network.

The impacts of DG on a low voltage (380/220 V (rms)) network were observed by analyzing voltage fluctuation, harmonic distortion, and voltage unbalance level verified at the PCC by (NUNES et al., 2017) through the assembly of a three-phase photovoltaic system in laboratory and a data acquisition system. The effects verified at the PCC when PV system injects power for penetration levels that vary from 0% to 40% of the nominal value, were used to assess the consequences to the grid, verifying significant changes in the variables studied (voltage fluctuation, harmonic distortion, and unbalanced level) as the power inserted by the photovoltaic system increases. In addition, these effects have random behavior due to the intermittent character of the photovoltaic energy source.

The effects of DG on the harmonics of a system were verified in (SA'ED et al., 2017) taking into account the level of penetration, number of DG units and the local of installation through simulations in Simulink / MATLAB ®of an IEEE 13-bar system. Scenarios without DG, changes in the number of DGs inserted in the system and in the power and location of DG insertion were considered. The Total Harmonic Distortion (THD) measurements were compared with international standards, concluding that the values exceed the limits determined at the points where the DG is inserted. As a solution, the authors propose and simulate a harmonic filtering technique, using single and double tuned passive filters.

Voltage fluctuation in the power grid was studied in (CHENG et al., 2016) based on analysis of real data from two distribution circuits operating in California, simulated in the "Distribution Engineering Workstation" software using solar irradiance data to model the photovoltaic system and considering a circuit with variable loads and control devices, simulating different levels of PV and load penetration. The results were obtained through power flow executions using measurement data from one year of photovoltaic generation of the studied sites, acquired with the SCADA software. As a solution to the voltage variation, the article recommends changes in the PF of the photovoltaic system depending on the generation levels obtained, concluding that this variation can be used to compensate and control voltage levels.

In (ABRI; EL-SAALDANY; ATWA, 2008), a rural distribution system of 41 buses with a peak load of 16.18 MVA and a feeder the system with a capacity of 300 A was studied. The voltage values of the system's DGs with unitary PF were compared to DGs

with fixed PF values of 0.95 leading and 0.95 lagging, indicating that the reactive power, while the PF is leading, may increase the voltage stability margin due to the higher sensitivity between the voltage variation ratio and reactive power variation than in relation to the active power.

The reverse power flow in the network causes protection problems, leading the voltage compensators not to operate correctly, problems that must be taken into account in the distribution system. (MOHAMMADI; MEHRAEEN, 2017) studied the impacts of photovoltaic systems on a low voltage grid and the relationship between grid protection and the insertion of excess power by the DG, using load flow to simulate the system's operation. It was observed that the excess energy generated by PV systems provokes the activation of protection, causing a potential voltage collapse. Thus, a smart network protector relay (SNPR) is proposed, which has an operation similar to a regular network protector in all modes except for the Sensitive Trip mode. In the Sensitive Trip mode a regular Microprocessor Network Protector Relay (MNPR) detects a reverse power flow and initiates a trip assuming fault occurrence in the upstream feeder.

The stability and the voltage level in an electrical network are influenced by the location and dimensioning of the DG in the system and can be analyzed through the active power and voltage in a node of a system (PV curve) obtained in the load flow (ABRI; EL-SAALDANY; ATWA, 2008). A method of locating and dimensioning the DG units was proposed, testing the voltage sensitivity to the change of the injected power and selecting the most sensitive bars to install the DG units. The PV curve shows that the active power is directly proportional to the voltage and using the Jacobian matrix and power flow calculations, it is possible to obtain the relation between the active power variation injected by the DG and the voltage variation, that is, how much the active power influences the stability of the node voltage. Besides, depending on the location and the power factor of the DG inserted at a point, the PV curve can change, also changing the voltage stability.

Probabilistic methods for simulating the installation of DGs and determining the maximum number of DGs in a low voltage network were indicated by (CHEN et al., 2012) so that the voltage levels do not exceed the maximum and minimum limits. The Gibbs sampler algorithm, one of the Markov Chain Monte Carlo Methods, is used to generate three key parameters for allocation of the non-deterministic DGs: type, size, and location. The authors studied the worst case scenario, with minimum load and maximum DG power installation and performed various simulations with the Electromagnetic Transients Program (EMTP) to determine if a given allocation of DGs would produce voltage profile problems. The paper concludes that high amounts of DG power inserted on the network with adequate conditions (mainly of location) allow the voltage levels to stay within acceptable limits, and even with minimal DG penetration, there may be unacceptably low

or high voltages at specific loads when DG units are installed at the wrong location.

Some articles determine index-based methods for evaluating the bars (or nodes) in the network suitable for DG. In (CASTILLO; AGUILA; GONZáLEZ, 2016), voltage stability indexes were proposed, characterized by impedance, voltage and active and reactive power to evaluate the system's behavior, allowing the determination of the appropriate location for installing the DG. A 9-bar radial distribution system was used to assess the impact and the ideal DG power that the system requires using algebraic modeling software. Maximum and minimum generation intervals and a consumption demand characteristic of peak hours are considered, and two methods of stability analysis were used, LQP (line stability factor) and FSVI (fast voltage stability index), allowing to find the appropriate location for the insertion of the DG on the network. The authors also used the software GAMS to address issues of economic dispatch, establishing a relation of the level of optimum impact for the correct functioning of the system.

The sensitivity in terms of voltage limits to the insertion of a DG in PCCs was analyzed in (LIMA; GEHRKE, 2018), modeling circuits through the impedance matrix and based on Kirchoff's laws using ideal current sources representing the DG to propose indexes (sensitivity values) based on voltage and impedance. The study evaluated the influence of DG on the voltage levels of the PCCs of systems with 16 PCCs, calculating the admittance matrix of this system in the MATLAB ®software. The sensitivity indexes were developed with the data of the equivalent impedance in each PCC and its relation to the voltage variation in order to determine which points of the network support a greater capacity of active power injection to compensate the voltage levels, respecting the maximum and minimum levels determined in the current regulations. The results were satisfactory for the analysis of ideal allocation without the need to simulate the studied networks using software, by simply analyzing the impedance parameters of the network and the proposed indexes.

This work is a continuation of (LIMA; GEHRKE, 2018), and develops indexes based on the voltage profile of the grid when DGs are inserted with power factor variation, and impedance variation (of the load and line of the grid), to determine the PCCs that are sensitive to the insertion of DG, needing less parameters to perform this study when compared to the afore mentioned bibliography, as it does not require power flow calculations,probabilistic methods and algebraic modeling softwares.

Table 2.1 shows a summary of the bibliographic review.

Table 2.1 – Summary of the bibliographic review.

Work	**Methodology**	**Variables Analyzed**
NUNES et al, 2017	Assembly of a three-phase photovoltaic system in laboratory and a data acquisition system	Voltage fluctuation, harmonic distortion and voltage unbalance level verified at the PCC
SA'ED et al, 2017	Simulations in Simulink/Matlab	System's harmonics
CHENG et al, 2016	Real data analysis in a software, power flow simulations using solar irradiance data to model the PV system	PCC's voltage variation
MOHAMMADI; MEHRAEEN, 2017	Power flow simulation	Relation between voltage variation, DG insertion and reverse power flow and protection.
ABRI; EL-SAALDANY; ATWA, 2017	Power flow simulation	Influence that the location, PF variation and dimensioning of the DG has on the voltage profile.
CHEN et al, 2012	Probabilistic methods and simulation	Voltage profile
CASTILLO; AGUILA; GONZÁLEZ, 2016	stability indexes using algebraic modeling software	Impedance, voltage, active and reactive power

3 THEORETICAL REASONING

In this chapter, DG definitions and reference values for the grid voltage contained in the current standards for DG insertion are addressed, in addition to Kirchhoff's Laws and Norton's theorems used to calculate current values that can be used to regulate the voltage levels within the limits established. The Monte Carlo Method is also explained, as it was chosen to determine variations in load and line impedance values that represent the real variation values, to perform analysis on these parameters and the relation with the voltage variation and the proposed sensitivity indexes.

3.1 DISTRIBUTED GENERATION

The *Agencia Nacional de Energia Eletrica (ANEEL)*, defines distributed generation as the installation of small generators, usually from renewable sources or even using fossil fuels, located close to the electricity consumption centers (ANEEL, 2016). This type of generation differs from centralized generation, which is the type of generation with production in large power generating plants in appropriate locations, the vast majority located distant from consumers, requiring the use of transmission lines and networks for the distribution of energy by the energy utilities, resulting in losses and decreased efficiency.

Within distributed generation, micro-generation and mini generation are also defined. The former being defined as the generation of electricity in a consumer unit with installed power less than or equal to 75 kW connected to the distribution network and using renewable sources or qualified co-generation. In comparison, the same type of installation characterizes the latter but covering limits of installed power depending on the source used, greater than 75 kW and less than or equal to 3 MW for water sources or less than or equal to 5 MW for other renewable energy sources or co-generation qualified, as (ANEEL, 2016), (ANEEL, 2012), (ANEEL, 2015).

The insertion of DG in the electric grid has brought some challenges to the Brazilian electricity system managers. In order to minimize these problems, regulatory standards have been developed by ANEEL and must be followed so that the standards established by the energy distributors are met by consumers who want to install DG. Additionally, the inverters used in the installations must follow the requirements provided in Brazilian and international standards to maintain the stability of the energy systems.

3.2 NATIONAL AND INTERNATIONAL TECHNICAL STANDARDS AND REGULATIONS

The International Electrotechnical Commission (IEC) is an international organization that determines and publishes international standards for electrical and electronic technologies. Within this context, the IEC 61727: 2004 and IEC 62116: 2014 standards regulate usage and operation standards for inverters in photovoltaic systems and establish requirements for the interconnection of photovoltaic systems with the distribution system (IEC, 2004), (IEC, 2014). IEC 62116: 2014 establishes test procedures to assess the performance of islanding prevention measures for photovoltaic systems.

In Brazil, technical standards (NBRs) are responsible for ensuring the quality, safety of equipment and people in photovoltaic installations (ZILES, 2018).

The technical standard NBR 16149 deals with the characteristics of the interface connecting DG (photovoltaic systems) to the electrical distribution network (ABNT, 2013). The inverters must meet the requirements of this standard in order to be connected to the electrical network, such as being within the limits of maximum and minimum voltage at the point of connection to the network, procedures that must be done in case of frequency variation, and THD injected of 5 %.

The *Procedimentos de Distribuição - PRODIST* are documents prepared by ANEEL to regulate and standardize the technical activities related to the functioning and performance of the electricity distribution systems. PRODIST's Module 8 deals with power quality problems, such as power factor, harmonics, voltage fluctuation, voltage imbalance, frequency variation and short-term voltage variation (ANEEL, 2018).

Regarding the power factor, the reference values at the connection point of the distributed generation defined are between 0.92 and 1.00 inductive or 1.00 and 0.92 capacitive for consumer unit or connection between distributors with voltage less than 230 kV. Concerning voltage levels, some limits are established on a permanent basis. The voltage to be contracted at the connection points with a nominal operating voltage below 230 kV must be between 95% and 105% of the nominal operating voltage of the system at the connection point (ANEEL, 2021). These limits were used as reference in the studies and simulations performed in this work's system.

3.3 THEORY OF ELECTRICAL CIRCUITS

3.3.1 Kirchhoff's Laws

Kirchhoff's Laws, used for analysis of electrical circuits, were introduced by the German physicist Gustav Robert Kirchhoff and are known as the Kirchhoff's Current Law (KCL or "knot" Law) and Kirchhoff's Voltage Law (KVL or mesh law) (ALEXANDER;

SADIKU, 2013).

The Kirchhoff's Current Law states that the sum of currents entering a node is equal to the sum of currents leaving that node. Mathematically, it can be represented using Equation (3.1):

$$\sum_{n=1}^{N} i_n = 0 \tag{3.1}$$

In which N is the number of branches connected to the node and i_n is the umpteenth current that enters or leaves the node (Figure 3.1).

Figure 3.1 – Representation of the Kirchhoff Law of Currents.

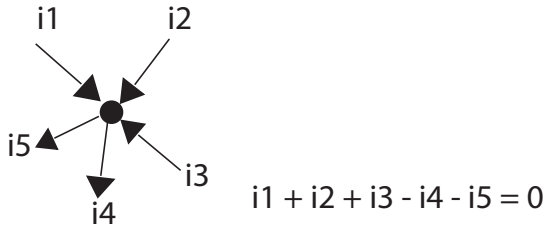

Source: The author.

The nodal analysis of a circuit is the application of KCL and consists of finding the voltages at the nodes of a circuit. KCL is applied to nodes in a circuit, using Ohm's Law to express currents in branches in terms of nodal voltages. Ohm's Law in phasor form is given by Equation (3.2).

$$\mathbf{Z} = \frac{\mathbf{V}}{\mathbf{I}} \tag{3.2}$$

$\boldsymbol{V}$ being the voltage, $\boldsymbol{I}$ being the current and $\boldsymbol{Z}$ being the impedance.

3.3.2 Norton's Theorem

Norton's Theorem states that a linear circuit with two terminals can be replaced by an equivalent circuit formed by a current source I_N in parallel with an impedance Z_N, where I_N is the short-circuit current through the terminals and Z_N is the input impedance or equivalent at the terminals when the independent sources are turned off (Figure 3.2) (ALEXANDER; SADIKU, 2013).

Figure 3.2 – Norton's Theorem.

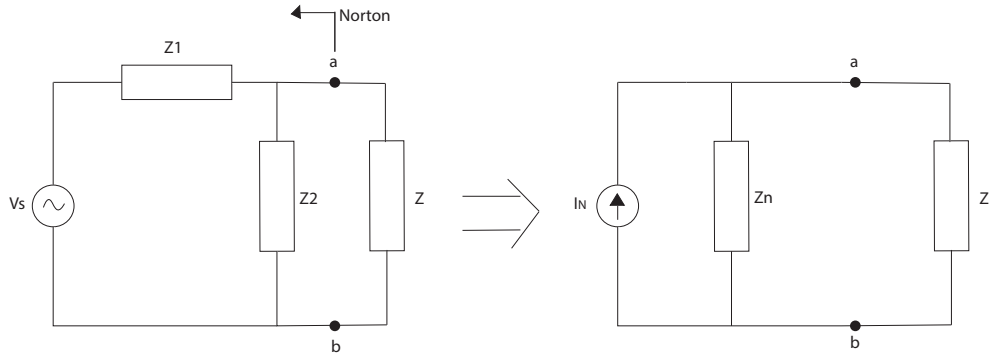

Source: The author.

For the substitution to occur, a and b being the terminals to which the theorem will be applied, the short-circuit current (Equation (3.3)) and the impedance seen at the output terminals are calculated, according to Equation (3.4), as shown in Figure 3.3.

Figure 3.3 – Norton's Theorem Equivalent.

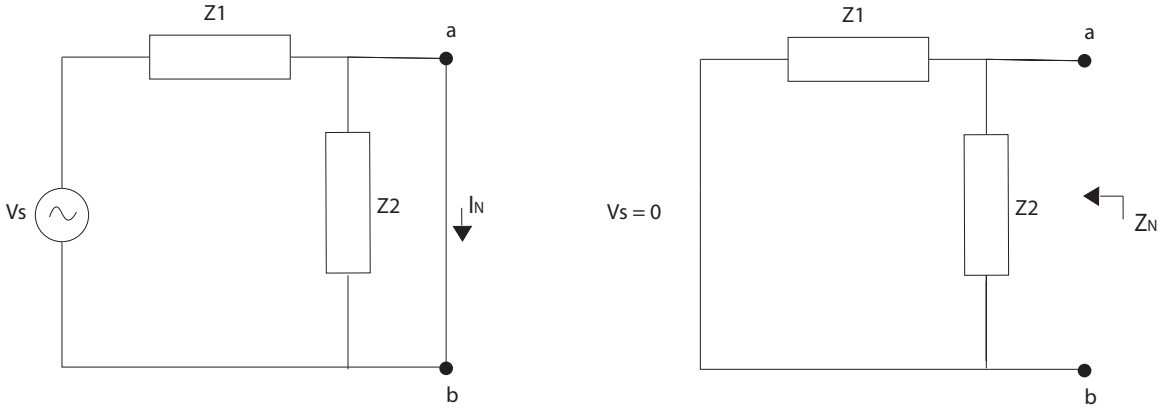

Source: The author.

$$I_N = \frac{\mathbf{Vs}}{\mathbf{Z1}} \tag{3.3}$$

$$Z_N = \frac{\mathbf{Z1Z2}}{\mathbf{Z1+Z2}} \tag{3.4}$$

Thus, Norton's theorem is equivalent to the transformation of sources, where a voltage source in series with an impedance can be replaced by a current source in parallel with the equivalent impedance at the terminals where the theorem is applied.

3.4 MONTE CARLO METHOD

The Monte Carlo method is a numerical method for solving deterministic problems by random sampling to make numerical estimations and model situations with many

variables involved.

The name is inspired by the casinos in Monte Carlo, Monaco, and it uses sequences of random numbers to build a sample of a population making it possible to obtain statistical estimates for solving problems (PAULA, 2014).

The main principle of the Monte Carlo method is the Law of Large Numbers, which is:

"As the number of identically distributed, randomly generated variables increases, their sample mean (average) approaches their theoretical mean."

Since it can be easily implemented, this method is used to obtain numerical approximations of complex functions through samples obtained with the help of probability functions, building a stochastic model by the method of statistical trials (PEASE, 2017).

Its application is used in several areas of knowledge, such as finance, engineering, computer graphics, medicine and astrophysics.

It is known that the behavior of an electrical network depends on stochastic variables, so voltages and currents will be different according to the load, that is, the number of people in the houses, industries, location and power of photovoltaic panels, among others (NAVARRO; OCHOA; RANDLES, 2013). One way to simulate this variable characteristic is through a Monte Carlo analysis, used in the methodology of this work. An algorithm for obtaining random load and generation values is run hundreds of times, for each situation presented, using the "rand" function in MATLAB ®.

4 METHODOLOGY AND MODELING

The modeling of the electrical circuits used for analysis in this work was based on Kirchhoff's Laws and Ohm's Law and on the determination of the impedance matrix of the circuits.

4.1 METHODOLOGY

Kirchhoff's Current Law (Equation (4.1)) in matrix form can be used to determine the voltage at a specific point in a circuit.

$$\boldsymbol{Y_{N\times N}} \cdot \boldsymbol{V_{N\times 1}} = \boldsymbol{I_{N\times 1}} \tag{4.1}$$

In which:
$\boldsymbol{Y_{N\times N}}$ is the admittance matrix;
$\boldsymbol{V_{N\times 1}}$ is the voltages matrix;
$\boldsymbol{I_{N\times 1}}$ the currents matrix;
and N is the maximum number of PCCs in the circuit.

The terms of the main diagonal of $\boldsymbol{Y_{N\times N}}$ must contain the sum of all admittances directly connected to the corresponding node, and the non-diagonal terms must contain the negative sum of all directly connected admittances between the corresponding nodes. The flowchart illustrated in Figure 4.1 represents the algorithm to determine the admittance matrix.

Figure 4.1 – Flowchart of algorithm of the admittance matrix determination.

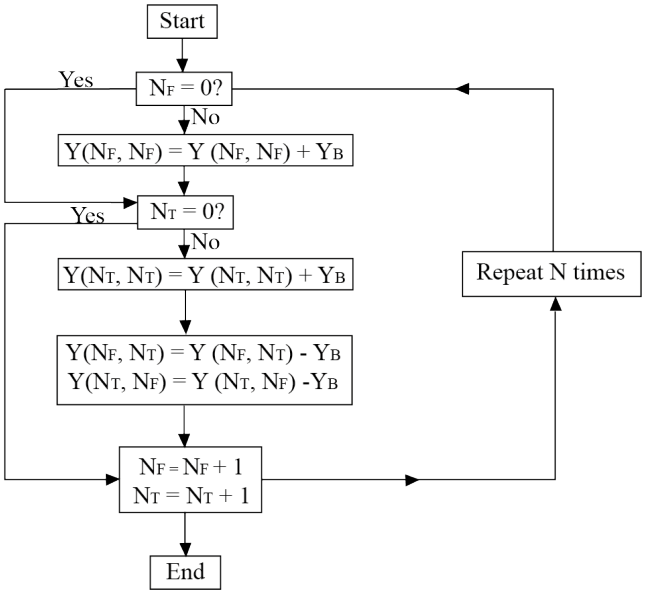

Source: The author.

In which:
N_F is the "node FROM";
N_T is the "node TO" the PCC;
N is the maximum number of PCCs in the circuit;
Y_B is the admitance in the node, or the node's load admittance.

To determine the equivalent impedance of a point in the system, we simply invert the admittance matrix, obtaining the impedance matrix as follows:

$$\boldsymbol{Z_{N\times N} = (Y_{N\times N})^{-1}} \tag{4.2}$$

The equivalent impedance of the "n" point is given by the term $\boldsymbol{Z(n,n)}$ and the influence that the DG inserted on the PCC *"n"* has in another point *"m"* is given by term $\boldsymbol{Z(n,m)}$. "n" and "m" varies from 1,...N, where "m" is different from "n".

The DG is often used to generate the maximum power to the consumer and can be installed to inject active power into the network. Thus, it can be modeled as an ideal current source and, in this case, have a small internal impedance that can be neglected (PEYGHAMI et al., 2017). In photovoltaic panels, the Maximum Power Point Trackers (MPPTs) are responsible for finding the maximum active power, or the optimal reference power to be injected into the network. The reactive power is calculated according to the desired power factor or is determined by the operator of the distribution network or the power distribution company. However, the interaction of the DG operating in maximum power, connected to grid, can generate overvoltage and even reverse power flow depending on the load profile. One way to prevent the overvoltage is constrain the maximum power depending on the PCC.

As the DG can be represented by an ideal current source, therefore the voltage level at a certain point is calculated using the Equation 4.3. The reference voltage is given by the network at the PCC of the main generation source (centralized generation). Thus, in this study, the DGs are inserted in the circuit as calculated ideal current sources to regulate the voltage levels, to reach 1.0 pu.

$$\boldsymbol{I_n = \frac{V^* - V_n}{Z(n,n)}} \tag{4.3}$$

where:
$\boldsymbol{I_n}$ is the phasor of the DG current at the node "n", with I_n being the amplitude and δ_n the angle;
$\boldsymbol{V}^*$ is the phasor of the reference voltage, $V^*\angle\theta^*$, V^* is the amplitude (usually 1.0 pu) and θ^* is the angle;
$\boldsymbol{V}_n$ is the phasor of the PCC voltage before the insertion of the DG, $V_n\angle\theta_n$, with V_n being

the amplitude and θ_n is the angle;
$\boldsymbol{Z(n,n)}$ is the complex phasor of the equivalent impedance at PCC *"n"*.

From Equation (4.3), it is possible to state that the maximum current, to prevent overvoltage, is provided for a voltage variation at a given $\boldsymbol{V}_n$ considering a fixed reference voltage $\boldsymbol{V}^*$=1 pu. Thus, the maximum power DG, in a given PCC "n", can be calculated with Equation 4.4.

$$\boldsymbol{S_n^{max} = Z(n,n)\overline{I}_n^2} \tag{4.4}$$

where $\overline{\boldsymbol{I}}$ denotes the complex conjugate of $\boldsymbol{I}$.

4.2 ANALYZED SYSTEM

Simulations were carried out in a 16 PCCs circuit, Figure 4.2, in order to identify a pattern. The circuit data was obtained in (GRADY; SAMOTYJ; NOYOLA, 1991), where point 1 is the source, points 2 to 9 represent branch 1 and points 10 to 16 represent branch 2. The voltage source ($\boldsymbol{E}_g$) is 1.0 pu, 60 Hz, internal impedance $\boldsymbol{Z}$ = 0.0031 + 0.0675i Ω, with R = 3.12 mΩ and L = 0.17913 mH. An array was created to insert the current sources data and the voltage source of 1.0 pu was replaced by a current source using Norton's Theorem, to be inserted in the currents array and enabling the use of the flowchart from Figure 4.1.

Figure 4.2 – 16 PCCs circuit using PI segments.

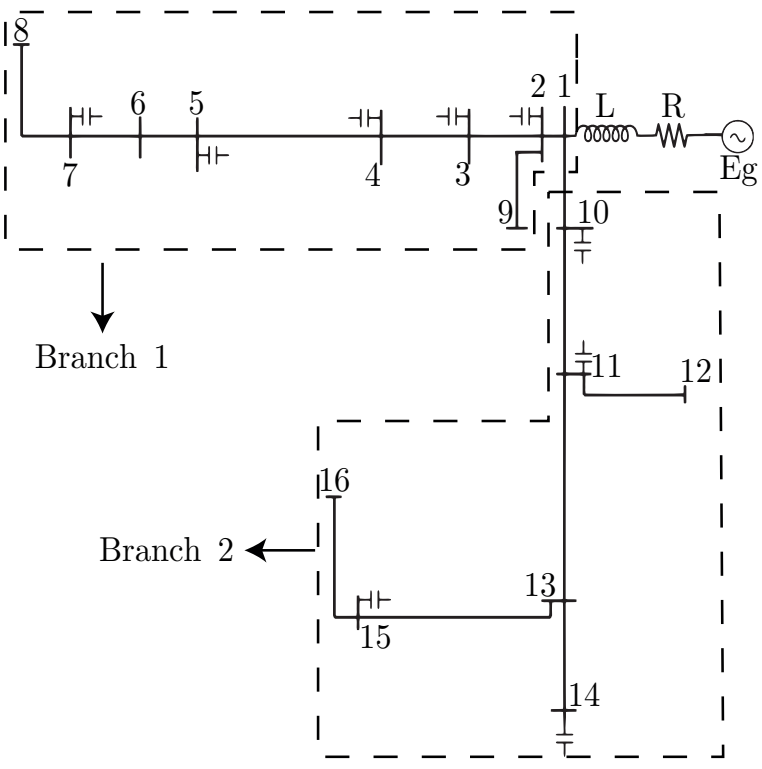

Source: (GRADY; SAMOTYJ; NOYOLA, 1991).

The parameters used in the system are available in Tables 4.1 and 4.2.

Table 4.1 – Parameters used - 16 PCCs circuit.

NF	NT	R (mΩ)	X_L (mΩ)	X_C (μS)
1	2	4.31	12.04	35.00
2	3	6.01	16.77	49.00
3	4	3.16	8.82	26.00
4	5	8.96	25.02	73.00
5	6	2.95	8.24	24.00
6	7	17.20	21.20	46.00
7	8	40.70	30.53	51.00
2	9	17.06	22.09	43.00
1	10	29.10	37.68	74.00
10	11	22.22	28.77	56.00
11	12	48.03	62.18	122.00
11	13	39.85	51.60	101.00
13	14	29.10	37.68	74.00
13	15	37.27	45.93	100.00
15	16	22.08	27.20	59.00

Table 4.2 – Load parameters used - 16 PCCs circuit.

PCC	P	Q	Shunt
1	0	0	0
2	0.0200	0.0120	-0.1050
3	0.0400	0.0250	-0.0600
4	0.1500	0.093	-0.0600
5	0.3000	0.2260	-0.1800
6	0.0800	0.0500	0
7	0.0200	0.0120	-0.0600
8	0.1000	0.0620	0
9	0.0500	0.0310	0
10	0.1000	0.0620	-0.0600
11	0.0300	0.0190	-0.1200
12	0.0200	0.0120	0
13	0.0800	0.0500	0
14	0.0500	0.0310	-0.1500
15	0.1000	0.0620	-0.0900
16	0.0200	0.0120	0

The system illustrated in Figure 4.2 was analysed in situations of variation of power factor of one DG inserted, overvoltage and multiple DGs inserted. The pattern stated to compare the results of these situations was the voltage values of the system with no DGs inserted. These four scenarios were simulated but many more scenarios can be simulated and analyzed, depending on the objective of the work. For this work, these four scenarios were chosen to observe and select the most sensistive PCCs to apply the sensitivity indexes, as can be seen further, on Chapter 5.

The four scenarios were:

#1 With one current source calculated with a reference voltage of V^*=1.0 pu at PCC 8;

#2 With one current source calculated with a reference voltage of V^*=1.05 pu at PCC 8;

#3 With one current source calculated with a reference voltage of V^*=1.0 pu at PCC 8 with different PFs (0.92 and 0.85 leading and lagging);

#4 With multiple current sources calculated with a reference voltage of V^*=1.0 pu.

5 SENSITIVITY INDEXES

After the simulation of the four scenarios mentioned in the Chapter 4 and results obtained, sensitivity indexes were proposed to analyze and determine the location where the insertion of DG could have more or less impact on the system, that is, the most sensitive PCC. The indexes are based on the equivalent impedance of the point which it was connected, the voltage levels before and after the insertion of the generation in many points of the circuit (especially where it was inserted) and the power factor of the DG.

5.1 VOLTAGE SENSITIVITY INDEX (VSI)

A voltage sensitivity index KV_n was developed to analyze the influence of the DG on the PCC of the circuits using Equation (5.1), correlating the equivalent impedance of the system and the voltage variation due to the generation insertion, the indexes is given as follows:

$$KV_n = \frac{\Delta V_n}{|\boldsymbol{Z(n,n)}|} \tag{5.1}$$

Where ΔV_n is the voltage variation on the PCC between the values obtained before and after the insertion of the DG; $\mathbf{Z(n,n)}$ is the equivalent impedance of the PCC.

5.1.1 Analysis Voltage Sensitivity Index

Since the system has two branches, one PCC from each branch was chosen randomly for the insertion of DGs, PCCs 5 (branch 1) and 11 (branch 2). The results for the application of the voltage sensitivity index in these two points are shown on Tables 5.1 and 5.2.

Table 5.1 – Voltage Sensitivity Index (VSI) with DGs in PCC 5 - complex circuit.

PCC	$\|\mathbf{Z(n,n)}\|(\Omega)$	ΔV_n	K_{Vn}
1	0.0675	0.0039	0.0573
2	0.0794	0.0073	0.0918
3	0.0958	0.0119	0.1237
4	0.1044	0.0143	0.1362
5	0.1293	0.0210	0.1621
6	0.1377	0.0210	0.1521
7	0.1627	0.0210	0.1286
8	0.2053	0.0208	0.1015
9	0.1046	0.0073	0.0693
10	0.1106	0.0039	0.0348
11	0.1456	0.0039	0.0267
12	0.2226	0.0039	0.0175
13	0.2086	0.0039	0.0187
14	0.2574	0.0039	0.0151
15	0.2662	0.0038	0.0143
16	0.3011	0.0038	**0.0128**

Table 5.2 – Voltage Sensitivity Index (VSI) with DGs in PCC 11 - complex circuit.

PCC	$\|\mathbf{Z(n,n)}\|(\Omega)$	ΔV_n	K_{Vn}
1	0.0675	-0.0118	-0.1740
2	0.0794	-0.0117	-0.1466
3	0.0958	-0.0116	-0.1209
4	0.1044	-0.0116	-0.1106
5	0.1293	-0.0115	-0.0890
6	0.1377	-0.0115	-0.0834
7	0.1627	-0.0115	-0.0704
8	0.2053	-0.0114	-0.0554
9	0.1046	-0.0117	-0.1114
10	0.1106	-0.0004	-0.0038
11	0.1456	0.0082	0.0565
12	0.2226	0.0082	0.0369
13	0.2086	0.0082	0.0394
14	0.2574	0.0082	0.0320
15	0.2662	0.0081	0.0305
16	0.3011	0.0081	**0.0271**

From analysis, the higher ΔV_n and lowest K_{Vn} is the most sensitive point of the circuit. In both cases it is PCC 16 ($K_{V16} = 0.0128$ and 0.0271).

5.1.2 Voltage Analysis with Power Factor Variation

Two points were chosen to analyze the influence of the PF variation in the grid, PCCs 7 and 15, one from each branch of the grid, and DGs with PF 0.85 and 0.92 leading and lagging are inserted individually. The power factor was changed to analyze the effects on the voltage levels of the circuit and to relate the voltage with the variation. The currents were calculated to regulate the voltage levels to 1.0 pu, using Equation (4.3).

A power factor sensitivity index (PFSI) K_{FPn} was then proposed to analyze the influence of the PF of the distributed generation on the system based on following Equation:

$$K_{FPn} = \frac{\Delta V_n}{FP} \tag{5.2}$$

Where ΔV_n is the PCC voltage variation before and after the DG insertion; Note that, the PF is the cosine of the difference between the angle of the PCC voltage and the DG angle.

Tables 5.3 and 5.4 show the result of applying the sensitivity index by power factor for each point of the network after insertion of the DG.

Table 5.3 – PF Sensitivity Index (PFSI) for PF Variation with DGs on PCC 7.

-	Power Factor			
-	Leading		Lagging	
PFSI	0.85	0.92	0.85	0.92
k1	-0.0151	0.0253	-0.0244	0.0096
k2	-0.0155	0.0320	-0.0265	0.0119
k3	-0.0163	0.0410	-0.0295	0.0148
k4	-0.0167	0.0457	-0.0312	0.0164
k5	-0.0182	0.0590	-0.0361	**0.0207**
k6	-0.0187	0.0635	-0.0378	**0.0222**
k7	-0.0127	0.0820	-0.0348	**0.0278**
k8	-0.0126	0.0815	-0.0346	**0.0276**
k9	-0.0155	0.0320	-0.0265	0.0118
k10	-0.0150	0.0252	-0.0242	0.0095
k11	-0.0150	0.0252	-0.0241	0.0096
k12	-0.0149	0.0252	-0.0241	0.0096
k13	-0.0148	0.0251	-0.0240	0.0096
k14	-0.0149	0.0252	-0.0241	0.0096
k15	-0.0149	0.0249	-0.0240	0.0094
k16	-0.0148	0.0250	-0.0239	0.0095

Table 5.4 – PF Sensitivity Index (PFSI) for PF Variation with DGs on PCC 15.

-	Power Factor			
-	Leading		Lagging	
PFSI	0.85	0.92	0.85	0.92
k1	-0.0102	0.0177	-0.0166	0.0241
k2	-0.0101	0.0177	-0.0165	0.0240
k3	-0.0100	0.0176	-0.0164	0.0239
k4	-0.0100	0.0175	-0.0164	0.0238
k5	-0.0100	0.0174	-0.0162	0.0235
k6	-0.0100	0.0174	-0.0162	0.0235
k7	-0.0099	0.0174	-0.0161	0.0235
k8	-0.0099	0.0173	-0.0160	0.0234
k9	-0.0101	0.0177	-0.0165	0.0240
k10	-0.0037	0.0397	-0.0136	0.0495
k11	0.0010	0.0563	-0.0118	0.0689
k12	0.0010	0.0562	-0.0116	0.0688
k13	0.0093	0.0857	-0.0084	**0.1032**
k14	0.0093	0.0860	-0.0084	**0.1034**
k15	0.0177	0.1126	-0.0042	**0.1345**
k16	0.0178	0.1126	-0.0041	**0.1344**

Inserting the DGs with different PFs has a more significant influence on the points of the same branch in which the DG is inserted. For DG in point 7, PCCs 6 and 8 have higher indexes, as well as points 1 to 5, when compared to the PCCs in branch 2. The same occurs for the insertion of current at point 15, PCCs 14 and 16 have higher indexes. The highest indexes indicate the most sensitive points for each case. Additionally, the points closest to the DG insertion also have higher equivalent impedance, as seen previously, which also influences the sensitivity.

5.1.3 Impedance Sensitivity Index (ISI)

The impedance sensitivity index KZ_n only needs the PCC impedance, and it is calculated as:

$$K_{Z_n} = \frac{|\boldsymbol{Z(n,n)}| - |\overline{\boldsymbol{Z}}|}{|\overline{\boldsymbol{Z}}|}, \tag{5.3}$$

Where: $\overline{\mathbf{Z}}$ is the average impedance of the system, considered as reference to calculate the impedance difference of each PCC related to all the PCCs of the system, obtained through the admittance matrix.

The sensitivity of each point is obtained using the impedances, as well as how much the insertion of a DG in a point of the grid affects the other points.

5.1.4 Analysis Impedance Sensitivity Index

The values of the impedance sensitivity index for the tested circuit are presented in Table 5.5. Each result was obtained in the point of installation. The mean ($\overline{\boldsymbol{Z}}$) and median ($\widetilde{\boldsymbol{Z}}$)can be used to determine the most, average and least sensitive PCCs in the grid.

Table 5.5 – Impedance Sensitivity Index (ISI).

PCC	$\mathrm{Re}\{\boldsymbol{Z}_{(n,n)}\}$	$\overline{\boldsymbol{Z}}$	$K\overline{Z}_n$	$\widetilde{\boldsymbol{Z}}$	$K\tilde{Z}_n$
1	0.0083	0.0698	-0.8812	0.0489	-0.8303
2	0.0138	0.0698	-0.8038	0.0489	-0.7198
3	0.0215	0.0698	-0.6950	0.0489	-0.5644
4	0.0255	0.0698	-0.6378	0.0489	-0.4826
5	0.0366	0.0698	-0.4788	0.0489	-0.2556
6	0.0398	0.0698	-0.4316	0.0489	-0.1881
7	0.0574	0.0698	-0.1796	0.0489	0.1718
8	0.0974	0.0698	0.3931	0.0489	0.9898
9	0.0309	0.0698	-0.5590	0.0489	-0.3701
10	0.0405	0.0698	-0.4201	0.0489	-0.1718
11	0.0654	0.0698	-0.0636	0.0489	0.3374
12	0.1134	0.0698	0.6222	0.0489	1.3170
13	0.1093	0.0698	0.5635	0.0489	1.2331
14	0.1412	0.0698	1.0217	0.0489	1.8875
15	0.1480	0.0698	1.1176	0.0489	2.0245
16	0.1699	0.0698	1.4326	0.0489	2.4744

From the analysis of Table 5.5, the PCCs which the sensitivity index is negative are the least sensitive and the points that have a positive index are the most sensitive to the insertion of DG, and they also have the highest equivalent impedance indicating that even a small current when inserted may cause a voltage variation above the limit allowed. In this way, it is possible to analyze which PCCs are more sensitive through the impedance sensitivity index, without the need to analyze other parameters. The most sensitive PCCs are 8, 12, 13, 14, 15 and 16, based on mean impedances $\overline{\boldsymbol{Z}}$, PCCs 7 and 11 are the average sensitive based on the index median $\widetilde{\boldsymbol{Z}}$ and the others are the lowest.

It is worth enlightening also, that the most sensitive PCC can be determined by the $\mathrm{Re}\{\boldsymbol{Z}_{(n,n)}\}$ and not from the impedance's module. The DG's current amplitude is low if the module or real part are high. However, the PCC that with the minimum current has the highest voltage variation is considered most sensitive point. Analyzing Tab 6.1 and individual currents, and considering the currents and impedances of PCCs 7 and 11, the sensitive order can be establish sorting the real part, where can be seen that the PCC 11 is more sensitive than PCC 7.

The real part $\mathrm{Re}\{\boldsymbol{Z}_{(n,n)}\}$ of the equivalent impedance obtained with the impedance matrix from the algorithm in Figure 4.1 was compared with the relation between the

voltage variation before and after the insertion of the DG and the current inserted in the PCC. The results are shown in Figure 5.1.

Figure 5.1 – Comparison between the real part of the PCC's impedance and the calculated using voltage and current values.

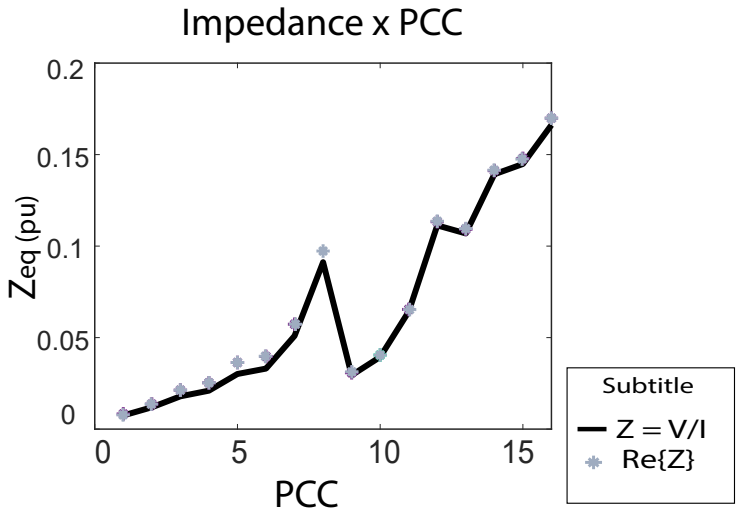

Source: the author.

As can be seen, the equivalent impedance curve of each PCC is very close to the points where the impedance was measured from the current and voltage results. This result corroborates with the efficiency and validates the algorithm used for the analysis of this work, in addition to demonstrating the relationship between the real part of the impedance and the sensitivity of the PCC, exposed above.

6 RESULTS

The equivalent impedance for the system's PCCs is given in Table 6.1.

Table 6.1 – Equivalent impedances resulted from the algorithm.

PCC	Real part	Imaginary part	Z(n,n)
1	0.0083	0.0670	0.0676∠82.9086°
2	0.0138	0.0783	0.0795∠79.9885°
3	0.0215	0.0937	0.0961∠77.0980°
4	0.0255	0.1016	0.1047∠75.9234°
5	0.0366	0.1243	0.1295∠73.6042°
6	0.0398	0.1321	0.1380∠73.2341°
7	0.0574	0.1524	0.1629∠69.3558°
8	0.0974	0.1809	0.2054∠61.7040°
9	0.0309	0.1001	0.1048∠72.8358°
10	0.0405	0.1028	0.1105∠68.4806°
11	0.0654	0.1298	0.1454∠63.2494°
12	0.1134	0.1913	0.2224∠59.3505°
13	0.1093	0.1768	0.2079∠58.2887°
14	0.1412	0.2143	0.2567∠56.6227°
15	0.1480	0.2197	0.2649∠56.0381°
16	0.1699	0.2465	0.2994∠55.4115°

The PCCs that are most sensitive to the insertion of the current source are the points with the highest absolute value of impedance (PCCs 7, 8, 12, 14, 15 and 16) since a small amount of current inserted will cause a high voltage variation. In these PCCs a small increase in the power and current injected by the DG causes a high increase in the voltage levels, and may even exceed the limits stipulated by current regulations.

The circuit illustrated in Figure 4.2 was simulated in four scenarios and compared with a reference scenario without a current source to correlate the sensitive PCCs with a pattern:

In the first scenario, one current source calculated with a reference voltage of V^*=1.0 pu was inserted at a PCC.

The current value required to set the PCC voltage level to 1 pu was calculated using Equation (4.3). The DG's PF is unitary, since the current is in phase with the V_n voltage of the PCC. In this scenario, PCC 8 was chosen as it has the highest impedance module

of branch 1 (see Table 6.1 line 8), and connecting a current source I8 = 0.3283∠−3.24° pu, the results are shown in Figure 6.1. As expected, the voltage is 1.0 pu after inserting the DG on PCC 8.

Because the impedance module is high, a small current was enough to regulate the voltage level. As shown in Figure 6.1, before the DG the voltage level at PCC n=8 was almost in the standards limits (V8=0.96) and, as expected, the voltage was 1.0 pu after the insertion of the DG. The voltage level in other PCCs has also increased, with greater variation in the PCC closest to where the DG was inserted. PCC 1, where the voltage source (generation) is, was not affected. Additionally, note that all the voltage levels form branch 1 have improved, and a small influence can be seen in branch 2.

Figure 6.1 – Voltages with DG on PCC 8.

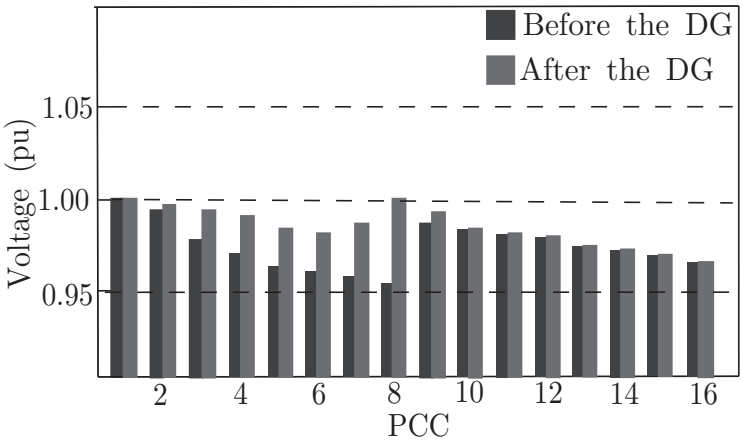

Source: the author.

To analyze the overvoltage problem, scenario #2, a current higher than necessary to regulate the voltage level to 1.0 pu was inserted by one DG at PCC 8. However the current was calculated based on Equation (4.3) with a reference value of 1.05 pu. The applied current was a little bit higher than the calculated $\boldsymbol{I_8} = \mathbf{0.6978}\ \angle 10.35°\ \mathbf{pu}$, in order to extrapolate the voltage standard. The values of the grid's voltages before and after the insertion of DG in every PCC are shown in Figure 6.2.

Figure 6.3 – Voltages with DG with different PFs inserted on PCC 8.

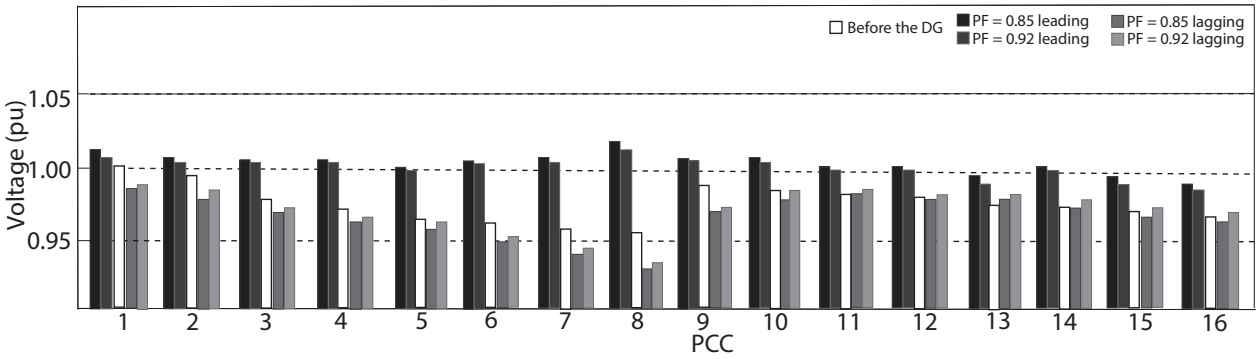

Source: the author.

Figure 6.2 – Voltages with DG on PCC 8 with amplitude value higher than calculated.

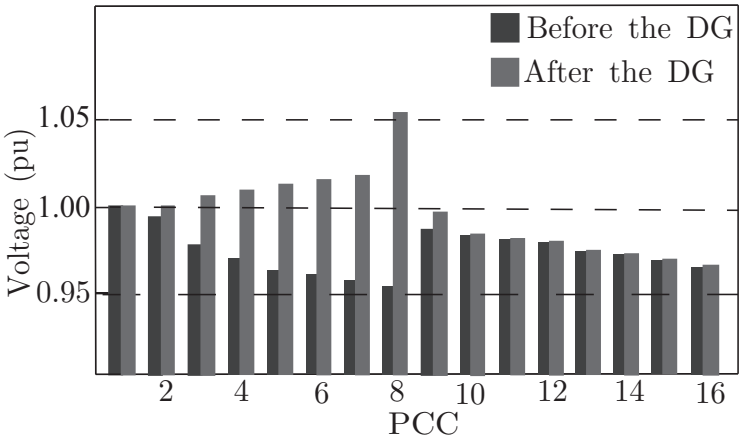

Source: the author.

For the same PCC 8, simulations were made for the insertion of DG with PF = 0.85 and 0.92 leading and lagging (scenario #3) and the currents were calculated so that the PCC would reach the same power as when DG has a unitary PF. The currents calculated were:

$$I_8 = 0.2791 \angle{-36.85^\circ} \text{ pu (fp = 0.85 leading)};$$
$$I_8 = 0.2791 \angle{139.80^\circ} \text{ pu (fp = 0.85 lagging)};$$
$$I_8 = 0.3020 \angle{-27.53^\circ} \text{ pu (fp = 0.92 leading)};$$
$$I_8 = 0.3020 \angle{147.90^\circ} \text{ pu (fp = 0.92 lagging)};$$

The results for the circuit's nodes voltages with different PFs for the same DG power are shown in Figure 6.3.

In the sequence, scenario #4 was simulated. Five DGs were connected at PCCs 5, 7, 11, 13 and 15, which were randomly chosen. Each DG current was calculated individually

for each point using Equation (4.3) with the reference voltage of V^*=1.0 pu. The DG currents calculated were:

$$I_5 = 0.8820 \angle 2.5474° \text{ pu};$$
$$I_7 = 0.7265 \angle 5.3966° \text{ pu};$$
$$I_{11} = 0.7563 \angle 19.3276° \text{ pu};$$
$$I_{13} = 0.6050 \angle 21.7914° \text{ pu};$$
$$I_{15} = 0.4981 \angle 22.5585° \text{ pu}.$$

The results of scenario #4 are shown in Figure 6.4.

Figure 6.4 – Voltages with DG on PCCs 5, 7, 11, 13 and 15.

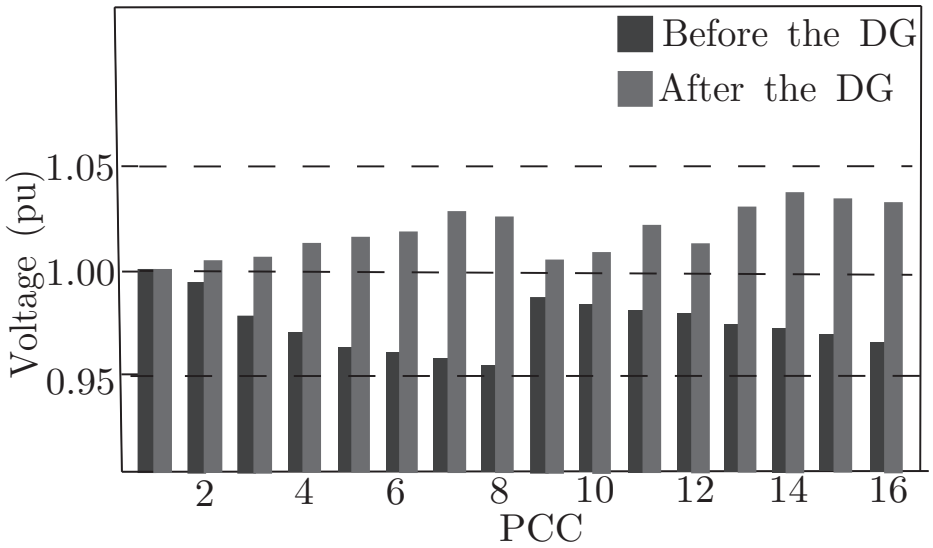

Source: the author.

When comparing Figures 6.1 and 6.4, it is noted that the voltage levels increased to values higher than 1.0 pu in the whole system, as shown in Figure 6.4. This is a result of the influence that the current sources inserted have in every point of the same branch as they were inserted, increasing the voltage in those points.

Note that the calculated current was 3 times greater than the previous to cause the overvoltage at point 8, that is, it has overreached the voltage limit of 1.05 pu. Depite having changed, the value of the current angle remained in phase with the voltage at the point, with the PF remaining unitary.

After examining the scenarios considering the current amplitude with unity PF, simulations were performed to evaluate the PF influence. The DG currents of some PCC were calculated separately using the Equation 4.3 and inserted in all PCCs simultaneously. Five PCCs were selected randomly to insert current sources (5, 7, 11, 13 and 15). In

Figure 6.5 – Voltages on the circuit when the DG with 0.85 lagging is inserted.

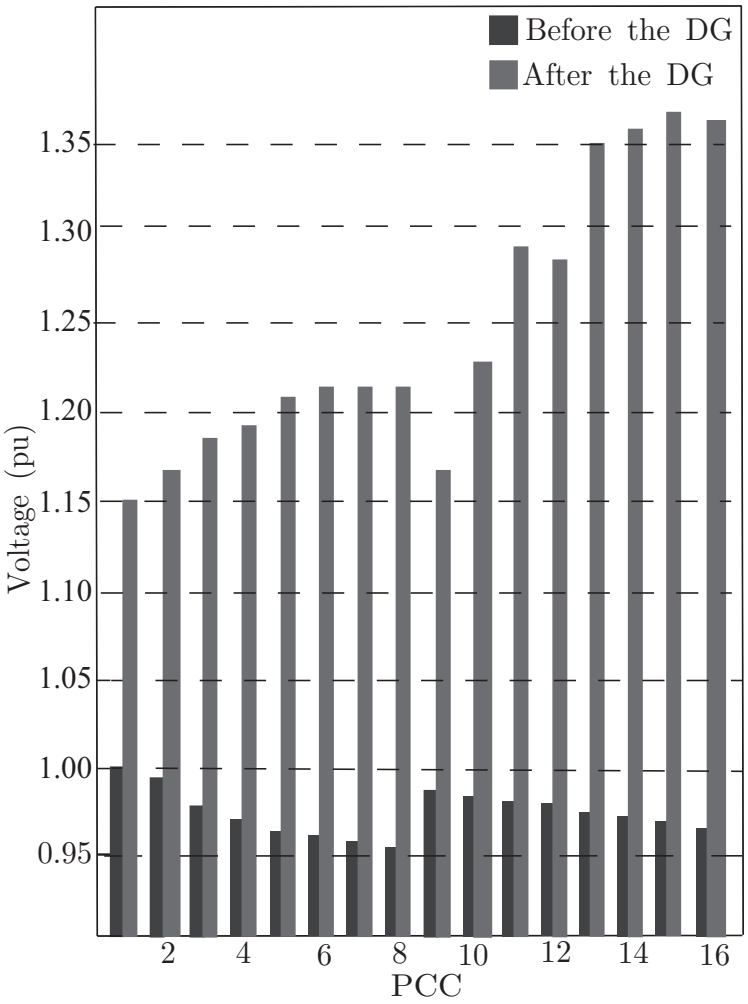

Source: the author.

Figures 6.5, 6.6, 6.7 and 6.8 the results of the circuit voltage values for the 0.85 and 0.92 leading and lagging power factors are presented.

The most sensitive PCCs vary according to where the DG is inserted and according to the power factor. Through the analysis of the simulations, it is noticed that if the PF is 0.85 and 0.92 lagging, the voltage levels are higher than the limit of 1.05 pu, when the PF is 0.85 leading some levels of voltage were below the minimum limit of 0.95 pu, with a voltage drop in the PCCs compared to when there was no current insertion.

The voltage of some PCCs increased, but within the limits of 0.95 and 1.05 pu. When a DG with PF of 0.92 leading is inserted, some voltage levels are lower than the minimum limit of 0.95 pu, causing a voltage drop compared to when there was no current source insertion. However, in some PCCs, the voltage level increased above the 1.05 pu maximum limit. The points of greatest voltage variation are most sensitive to the insertion of DG (PCCs 7, 8, 15 and 16). The simulation results confirm the effects of the PF variation on the grid and the importance of keeping the PF closer to the unit for the maintenance

Figure 6.6 – Voltages on the circuit when the DG with 0.85 leading is inserted.

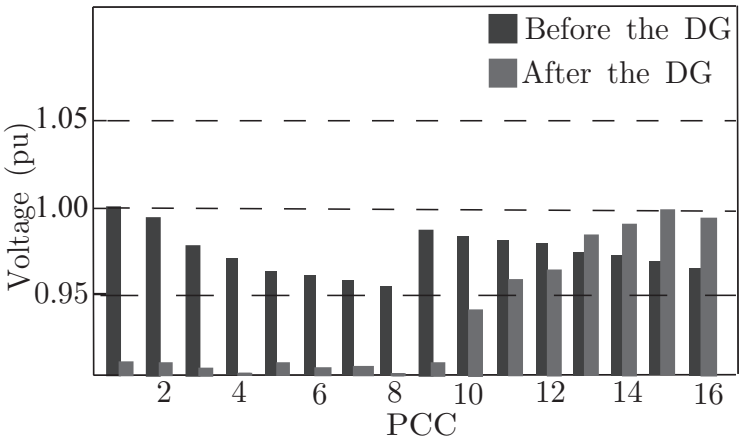

Source: the author.

Figure 6.7 – Voltages on the circuit when the DG with 0.92 lagging is inserted.

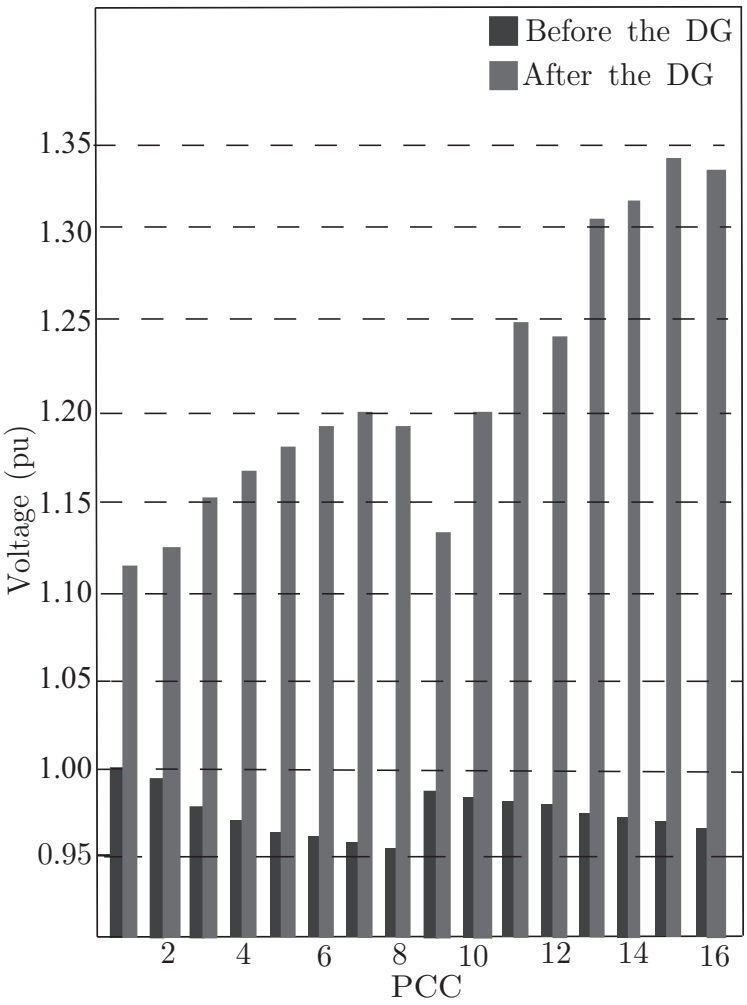

Source: the author.

Figure 6.8 – Voltages on the circuit when the DG with 0.92 leading is inserted.

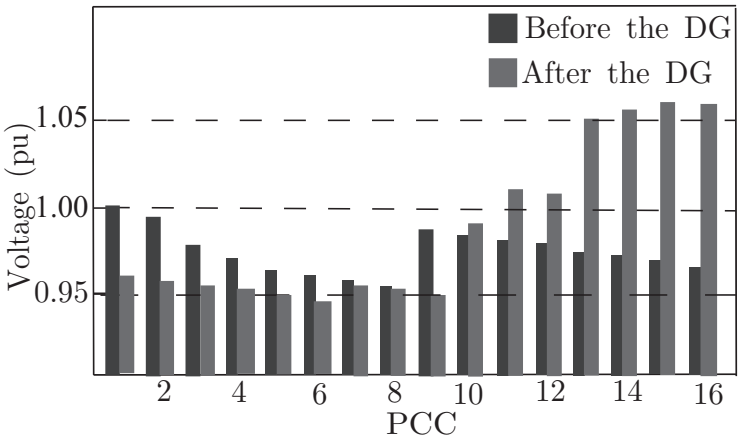

Source: the author.

of the voltage limits of the network.

For both leading PF values, at point 8, the voltage level remained about 1% above the reference value of 1 pu, and even the other points had an increase in the voltage level to a value above 1 pu but did not reach or exceed the maximum limit of 1.05 pu established by regulation, in this scenario, the maximum $\Delta V = 0.06$. As for the lagging PF, the voltage levels remained below the reference of 1 pu, and on PCCs 6, 7 and 8 even below the minimum limit value of 0.95 pu. As the power was determined from scenario #1 under unitary PF, it can be stated that even with lower PFs in leading, when analyzing just a single PCC, the voltage level does not exceed the standards. This can be corroborated because the maximum power for each point of the studied grid can be given from Equation (4.3).

However, even with several DGs, almost 30% of the PCCs with a maximum power current source to regulate V^*=1 pu, the values stayed between 0.95 and 1.05 pu, within the standard limits. Thus, it is possible to assume that considering the present regulation, in which the DG should operate with power factor (PF)=1, that the proposed strategy with maximum power for regulating each PCC to V^*=1 pu, can be used to evaluate the maximum DG penetration.

6.1 RESULTS UNDER IMPEDANCE AND LOAD VARIATIONS BASED ON MONTE CARLO SIMULATIONS

In the first simulations, the circuit impedance was considered constant in order to find a pattern. However, the grid is dynamic prone to load and line impedance changes over time. Thus, an analysis was performed based on the *Monte Carlo* method to get as close as possible to real results.

For the Monte Carlo tests, 100 variations were made for three scenarios. In each

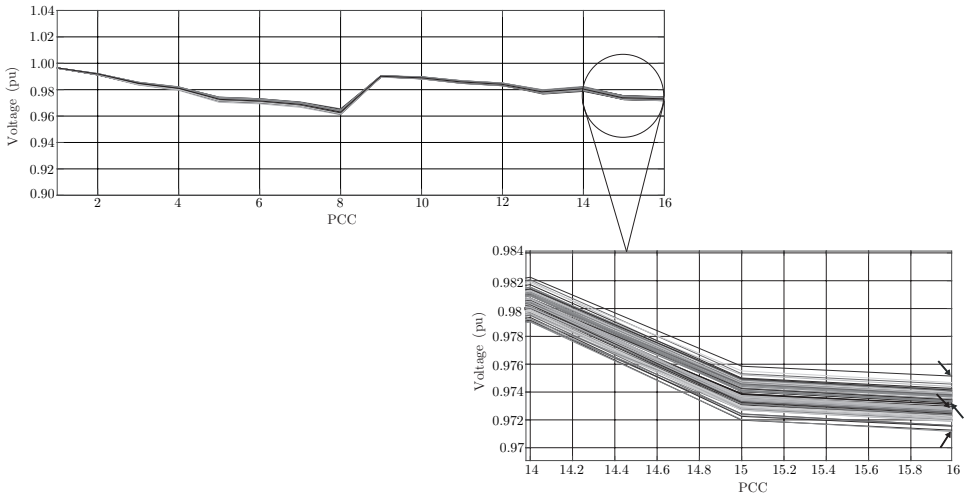

Figure 6.9 – Voltage variation under line impedance changing using the Monte Carlo method.

variation, random values of load and line impedance were generated within the range stipulated for each scenario. Thus, the large amount of random values generated makes it closer to obtaining an estimate of the real values of variation of each situation. These tests were made using the "rand" function in Matlab ®.

1. a variation of ± 10% was considered for the line parameters, as temperature changes;
2. a variation of ± 100 % was considered, as the load varies according to the demand;
3. a variation in both, ± 10% on the line parameters and ± 100 % on the load impedance parameters simultaneously.

The limit of 100% for the load was chosen based on the fact that the load varies depending on the consumers' demand, going from almost no load (0%) to a high load (100%). The variation of the line impedance parameters between the nodes is small due only to the losses caused by temperature variations, so the limit of 10 % was chosen.

The voltage variation that was simulated with the grid impedance is shown in Figures 6.9, 6.10 and 6.11 using the Monte Carlo method as mentioned before. The three cases were considered and it is possible to observe the higher variation on the PCCs of the second branch.

The highlight in PCC 8 and PCC 16 shows that the variation is greater for the most sensitive points, due to the high equivalent impedance of these PCCs.

Although the impedance influences the sensitivity, the variation of load and line parameters does not change (see lines 12 to 16 on Figures 6.12, 6.13, 6.14, the PCCs that are more sensitive to the insertion of DG. It is possible to note the change in the sensitivity values, but it does not imply a change in the order of the PCCs' sensitivity.

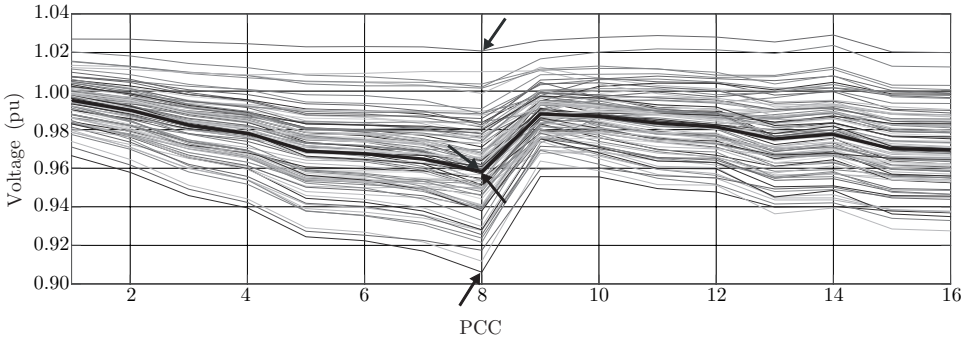

Figure 6.10 – Voltage variation under load changing using the Monte Carlo method.

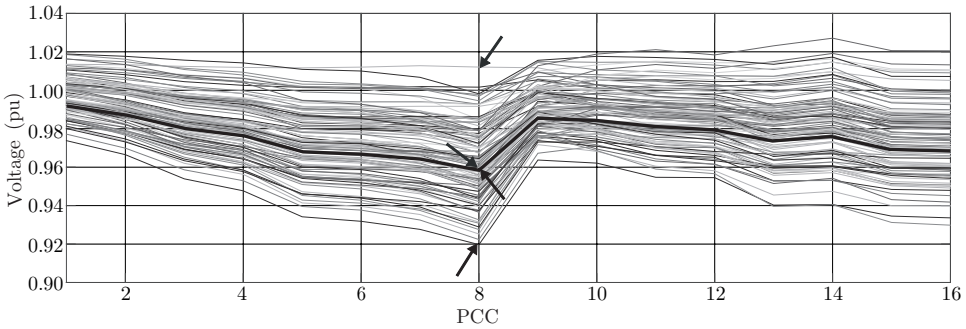

Figure 6.11 – Voltage variation under grid parameters changing (line and load impedance) using the Monte Carlo method.

For the case with a load variation, the PCCs 9, 4, 13 and 8 changed the order of sensitivity compared to the other impedance variations and when the impedance is constant, according to the values shown in Figure 6.14. However, as there are 4 PCCs and a small variation in values, it does not influence the use of the index to indicate the most sensitive points.

For the scenario with variation of 10 % in the line parameters and 100 % in the load simultaneously, there was a change in the sensitivity levels of PCCs 7, 9, 10 and 11 (Figure 6.15) but compared with Figure 6.14, with only the load variation, there was a change in the sensitivity level of PCC 11 indicating that the line impedance variation does not have as much influence on the sensitivity of most grid's PCCs as the load variation.

Figure 6.12 – Constant impedance.

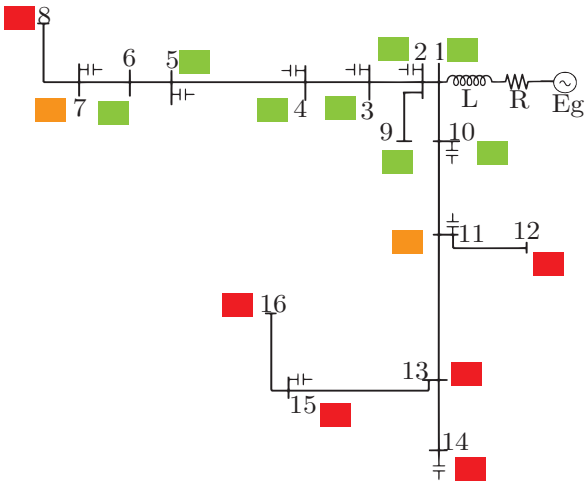

PCC	$\lvert Z \rvert$	$\overline{Z}$	$\widetilde{Z}$
1	0.0676	0.1617	0.1415
2	0.0787	0.1617	0.1415
3	0.0970	0.1617	0.1415
4	0.1062	0.1617	0.1415
5	0.1296	0.1617	0.1415
6	0.1390	0.1617	0.1415
7	0.1666	0.1617	0.1415
8	0.2095	0.1617	0.1415
9	0.1040	0.1617	0.1415
10	0.1125	0.1617	0.1415
11	0.1439	0.1617	0.1415
12	0.2266	0.1617	0.1415
13	0.2000	0.1617	0.1415
14	0.2514	0.1617	0.1415
15	0.2601	0.1617	0.1415
16	0.2944	0.1617	0.1415

Label:

- Low sensibility level: $Z < \widetilde{Z}$ and $Z < \overline{Z}$
- Medium sensibility level: $Z > \widetilde{Z}$
- High sensibility level: $Z > \overline{Z}$

Source: the author.

Figure 6.13 – Line impedance variation.

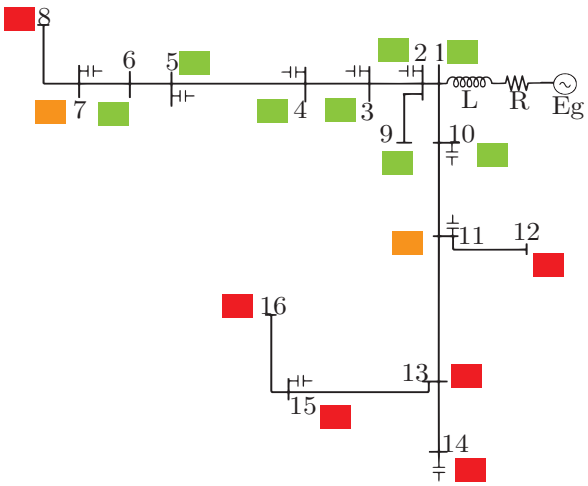

PCC	$\lvert Z \rvert$	$\overline{Z}$	$\widetilde{Z}$
1	0.0676	0.1634	0.1422
2	0.0795	0.1634	0.1422
3	0.0952	0.1634	0.1422
4	0.1039	0.1634	0.1422
5	0.1292	0.1634	0.1422
6	0.1372	0.1634	0.1472
7	0.1616	0.1634	0.1472
8	0.2068	0.1634	0.1472
9	0.1044	0.1634	0.1472
10	0.1104	0.1634	0.1472
11	0.1472	0.1634	0.1472
12	0.2235	0.1634	0.1472
13	0.2139	0.1634	0.1472
14	0.2645	0.1634	0.1472
15	0.2662	0.1634	0.1472
16	0.3040	0.1634	0.1472

Label:

- Low sensibility level: $Z < \widetilde{Z}$ and $Z < \overline{Z}$
- Medium sensibility level: $Z > \widetilde{Z}$
- High sensibility level: $Z > \overline{Z}$

Source: the author.

Figure 6.14 – Load variation.

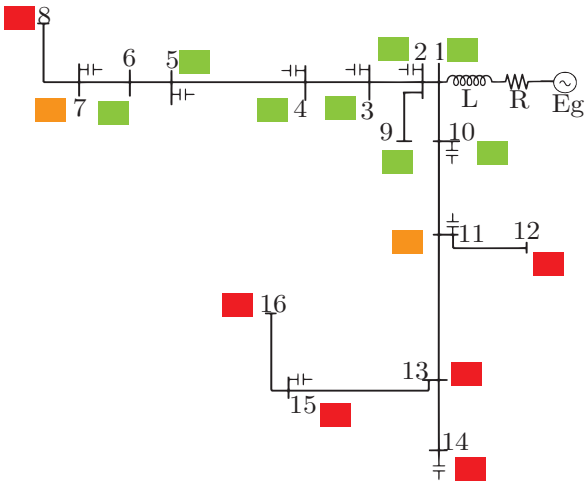

PCC	|Z|	$\overline{Z}$	$\widetilde{Z}$
1	0.0676	0.1617	0.1415
2	0.0787	0.1617	0.1415
3	0.0970	0.1617	0.1415
4	0.1062	0.1617	0.1415
5	0.1296	0.1617	0.1415
6	0.1390	0.1617	0.1415
7	0.1666	0.1617	0.1415
8	0.2095	0.1617	0.1415
9	0.1040	0.1617	0.1415
10	0.1125	0.1617	0.1415
11	0.1439	0.1617	0.1415
12	0.2266	0.1617	0.1415
13	0.2000	0.1617	0.1415
14	0.2514	0.1617	0.1415
15	0.2601	0.1617	0.1415
16	0.2944	0.1617	0.1415

Label:

- Low sensibility level: $Z < \widetilde{Z}$ and $Z < \overline{Z}$
- Medium sensibility level: $Z > \widetilde{Z}$
- High sensibility level: $Z > \overline{Z}$

Source: the author.

Figure 6.15 – Load and line variation.

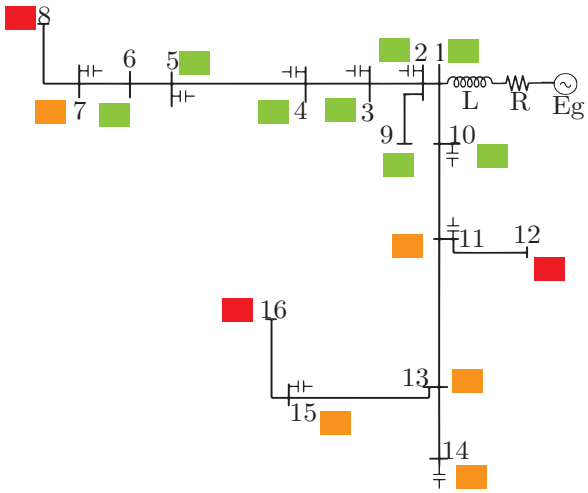

PCC	|Z|	$\overline{Z}$	$\widetilde{Z}$
1	0.0682	0.1637	0.1418
2	0.0796	0.1637	0.1418
3	0.0950	0.1637	0.1418
4	0.1030	0.1637	0.1418
5	0.1262	0.1637	0.1418
6	0.1344	0.1637	0.1418
7	0.1593	0.1637	0.1418
8	0.2043	0.1637	0.1418
9	0.1044	0.1637	0.1418
10	0.1114	0.1637	0.1418
11	0.1492	0.1637	0.1418
12	0.2223	0.1637	0.1418
13	0.2160	0.1637	0.1418
14	0.2617	0.1637	0.1418
15	0.2736	0.1637	0.1418
16	0.3101	0.1637	0.1418

Label:

- Low sensibility level: $Z < \widetilde{Z}$ and $Z < \overline{Z}$
- Medium sensibility level: $Z > \widetilde{Z}$
- High sensibility level: $Z > \overline{Z}$

Source: the author.

7 CONCLUSIONS

This work presents a methodology to verify the effects of DG in an electrical system using current sources. Sensitivity indexes have been proposed based on simulation results. It turns out that connecting the DG to a PCC affects PCCs in the same branch, and connecting multiple DGs not only regulates the voltage levels in the PCC that was inserted, but can also cause overvoltage in the other PCCs. In addition, the equivalent impedance of a PCC influences its sensitivity and the current required for voltage regulation. Three cases of line and load impedance variation were analyzed, and the PCCs of greater sensitivity did not change with these variations, although some PCCs in the circuit did change the sensitivity according to the proposed changes. An analysis was also made of the variation of the DG power factor, from 1.0 to 0.92 and 0.85 lagging and leading, showing that the sensitivity of the PCCs changes with this variation, and also changes according to the location where the DG is inserted.

With the presented indexes it is possible to analyze which points of installation of a DG cause more impact on the voltage levels of an electrical network, without the need for simulations. The impedance sensitivity index facilitates the analysis because the only necessary variable is the impedance of the network points, which is easy to obtain. The voltage sensitivity index contributes to the analysis of the voltage variation of electrical systems and the sensitivity index by power factor helps determining which points are most susceptible to voltage variation, according to the active and reactive power levels injected in the network by the DG. The proposed indexes can also be used as part of optimization algorithms for allocation and impact measurement of DG.

REFERENCES

ABNT. *Normas Técnicas Brasileiras. NBR 16149 - Procedimentos de Distribuição de Energia Elétrica no Sistema Elétrico Nacional – PRODIST*. 2013. Accessed August 4, 2019. Disponível em: <https://download.aldo.com.br/energy/2_Normas_Redes.pdf>.

ABRI, R.; EL-SAALDANY, E.; ATWA, Y. Optimal placement and sizing method to improve the voltage stability margin in a distributed system using distributed generation. *IEEE Transactions on Power Systems*, IEEE, p. 326–334, 2008.

ALEXANDER, C. K.; SADIKU, M. N. O. *Fundamentos de Circuitos Elétricos*. Reading, Massachusetts: McGraw Hill, 2013.

ANEEL. *RESOLUÇÃO NORMATIVA Nº 482, DE 17 DE ABRIL DE 2012*. 2012. Accessed August 4, 2019. Disponível em: <http://www2.aneel.gov.br/cedoc/bren2012482.pdf>.

_____. *RESOLUÇÃO NORMATIVA Nº 687, DE 24 DE NOVEMBRO DE 2015*. 2015. Accessed August 4, 2019. Disponível em: <http://www2.aneel.gov.br/cedoc/ren2015687.pdf>.

_____. *Cadernos Temáticos ANEEL: Micro e Minigeração Distribuída - Sistema de Compensação de Energia Elétrica*. 2016. Accessed August 4, 2019. Disponível em: <https://www.aneel.gov.br/documents/656877/14913578/Caderno+tematico+Micro+e+Minigera%C3%A7%C3%A3o+Distribuida+-+2+edicao/716e8bb2-83b8-48e9-b4c8-a66d7f655161?version=1.3#:~:text=Desde%2017%20de%20abril%20de%202012,%20quando%20a,para%20a%20rede%20de%20distribui%C3%A7%C3%A3o%20de%20sua%20localidade.>

_____. *Procedimentos de Distribuição de Energia Elétrica no Sistema Elétrico Nacional – PRODIST*. 2018. Accessed December 28, 2020. Disponível em: <https://www.aneel.gov.br/prodist>.

_____. *Procedimentos de Distribuição de Energia Elétrica no Sistema Elétrico Nacional – PRODIST: Módulo 8 – Qualidade da Energia Elétrica (Revisão 12)*. 2021. Accessed December 28, 2020. Disponível em: <https://www.aneel.gov.br/documents/656827/14866914/M%C3%B3dulo_8-Revis%C3%A3o_12/342ff02a-8eab-2480-a135-e31ed2d7db47>.

BARKER, P. P.; MELLO, W. R. d. *Determining the Impact of Distributed Generation on Power Systems: Part 1 - Radial Distribution Systems.* [S.l.]: Power Technologies, Inc., 2000.

CASTILLO, F.; AGUILA, A.; GONZáLEZ, J. Analysis of stability of tension and losses of electric power in distribution networks with distributed generation. *IEEE Latin America Transactions*, v. 14, n. 11, p. 4491–4498, 2016.

CHEN, P. et al. Analysis of voltage profile problems due to the penetration of distributed generation in low voltage secondary distribution networks. *IEEE Transactions on Power Delivery*, IEEE, p. 2020–2028, 2012.

CHENG, D. et al. Photovoltaic (pv) impact assessment for very high penetration levels. *IEEE Journal of Photovoltaics*, IEEE, p. 295–300, 2016.

GRADY, W. M.; SAMOTYJ, M. J.; NOYOLA, A. H. Minimizing network harmonic voltage distortion with an active power line conditioner. *IEEE Transactions on Power Delivery*, IEEE, p. 1690–1697, 1991.

IEC. *IEC 61727:2004 Photovoltaic (PV) systems - Characteristics of the utility interface*. 2004. Accessed December 11, 2019. Disponível em: <https://www.iecee.org/dyn/www/f?p=106:49:0::::FSP_STD_ID:5736>.

_____. *IEC 62116:2014 Utility-interconnected photovoltaic inverters - Test procedure of islanding prevention measures*. 2014. Accessed December 11, 2019. Disponível em: <https://webstore.iec.ch/publication/6479>.

LIMA, M. C.; GEHRKE, C. *Avaliação do impacto de geração distribuída baseada em fonte de corrente e impedância equivalente. XXII Congresso Brasileiro de Automática*, 2018.

MOHAMMADI, P.; MEHRAEEN, S. Challenges of pv integration in low-voltage secondary networks. *IEEE Transactions on Power Delivery*, IEEE, p. 525–535, 2017.

NAVARRO, A.; OCHOA, L. F.; RANDLES, D. Monte carlo-based assessment of pv impacts on real uk low voltage networks. In: . [S.l.: s.n.], 2013. p. 1–5.

NUNES, E. A. F. et al. Impact of pv systems on microgrids under different levels of penetration and operational scenarios. In: *2017 Brazilian Power Electronics Conference (COBEP)*. [S.l.: s.n.], 2017. p. 1–6.

PAULA, R. R. de. *Método de Monte Carlo e Aplicações*. Tese (*Monografia (Bacharel em Matemática com Ênfase em Matemática Computacional)*) — Universidade Federal Fluminense (UFF), 2014.

PEASE, C. *An Overview of Monte Carlo Methods*. 2017. Accessed January 11, 2021. Disponível em: <https://towardsdatascience.com/an-overview-of-monte-carlo-methods-675384eb1694>.

PEYGHAMI, S. et al. Grid synchronization for distributed generations. In: ABRAHAM, M. A. (Ed.). *Encyclopedia of Sustainable Technologies*. Oxford: Elsevier, 2017. p. 179 – 194. ISBN 978-0-12-804792-7. Disponível em: <http://www.sciencedirect.com/science/article/pii/B9780124095489101344>.

QI, S. et al. Analysis on voltage fluctuation of active distribution network containing wind-solar hybrid distributed generation. p. 168–173, Sep. 2018.

SA'ED, J. A. et al. Impact of integrating photovoltaic based dg on distribution network harmonics. In: *2017 IEEE International Conference on Environment and Electrical Engineering and 2017 IEEE Industrial and Commercial Power Systems Europe (EEEIC / I CPS Europe)*. [S.l.: s.n.], 2017. p. 1–5.

SCHWEITZER, E. O.; FINNEY, D.; V., M. M. Communications-assisted schemes for distributed generation protection. In: *PES T D 2012*. [S.l.: s.n.], 2012. p. 1–8.

SHAHZAD, U.; KAHROBAEE, S.; ASGARPOOR, S. Protection of distributed generation: Challenges and solutions. *Energy and Power Engineering*, v. 9, p. 614–653, 2017.

SOUZA, P. A. et al. Analysis of active and reactive power injection in distributed systems with photovoltaic generation. p. 1–6, May 2018.

WALLING, R. A. et al. Summary of distributed resources impact on power delivery systems. *IEEE Transactions on Power Delivery*, IEEE, p. 1636–1644, 2008.

ZILES, R. *NORMAS TÉCNICAS BRASILEIRAS, AVALIAÇÃO DE CONFORMIDADE E PROCEDIMENTOS DE CONEXÃO*. 2018. Accessed August 4, 2019. Disponível em: <https://www.aneel.gov.br/documents/656877/16832773/5+-+NORMAS+T%C3%89CNICAS+BRASILEIRAS.pdf/9aeffe7c-dcbf-49c7-f5a6-6d2880d9f9fe>.